University of Nevada, Reno

Enhancing End-User Water Quality through the Characterization of Reclaimed Wastewater and Modifications to Current Treatment Practices

A thesis submitted in partial fulfillment of the requirements for the degree of Master of Science in Civil and Environmental Engineering

by

Weston M. Helander

Dr. Eric A. Marchand/Thesis Advisor

May 2012

University of Nevada, Reno
Statewide • Worldwide

THE GRADUATE SCHOOL

We recommend that the thesis
prepared under our supervision by

WESTON M. HELANDER

entitled

Enhancing End-User Water Quality Through The Characterization Of Reclaimed Wastewater And Modifications To Existing Treatment Practices

be accepted in partial fulfillment of the
requirements for the degree of

MASTER OF SCIENCE

Eric A. Marchand, Ph.D., Advisor

Keith E. Dennett, Ph.D., Committee Member

Glenn Miller, Ph.D., Graduate School Representative

Marsha H. Read, Ph. D., Dean, Graduate School

May, 2012

Abstract

Up to half of all freshwater demand in certain regions of the United States is used for the irrigation of lawns and gardens, prompting the need for water reclamation and recycling in dry, arid cities. In order for reclaimed water to be successful, it must meet certain water quality criteria to satisfy the needs of end users. In recent years, reclaimed water from the South Truckee Meadows Water Reclamation Facility (STMWRF) has experienced challenges in meeting the quality criteria of its customers. The aim of this study was to monitor water quality in the Huffaker Hills Reservoir and determine the feasible options for the improvement of reclaimed water quality from STMWRF.

Treatment efficiencies in STMWRF's oxidation ditch and filtration media system were measured to assess the effects of cyclical aeration and chemical coagulation on effluent water quality, respectively. Additionally, weekly water quality analyses were performed to determine the seasonal changes associated with algae growth in various locations in the storage reservoir and reclaimed water distribution system. High nutrient concentrations in the reservoir allowed for significant algal activity, with the greatest activity occurring from June to September.

Cyclical aeration in the plant's oxidation ditch was found to have a severe impact on nutrient loading to the storage reservoir. Ammonia and phosphorus loadings to the reservoir could be reduced by as much as 78% and 40%, respectively, if the oxidation ditch were aerated continuously. Pilot-scale filtration tests were run using ferric chloride and aluminum sulfate (alum) as coagulants at various doses run in triplicate. Variation in removal of alum and ferric chloride at each dose narrowed as concentration increased, though it was difficult to accurately predict future removal efficiencies due to changes in influent water characteristics such as pH and turbidity.

Acknowledgements

This thesis was made possible by the aide and support of many people. I would like to acknowledge the Dr. Eric Marchand for his support and expert guidance over the course of this study. I would like to thank Washoe County for their support in funding this project, as well as John Hulett, Dwayne Smith, and Doug Barber for their assistance in developing sampling plans and testing procedures. Additional thanks go to Jennifer Damon, Shawnee Dunagan, George Gaynor, William (Boomer) Holmes, Jeff Kolledge, and Dante Lorenzetti for their help in the sampling process. A special thanks to Tony Dimpel and Viktoriya Weirauch for the assistance in the laboratory, as well as Katie Bowden, Emily Cole, Zach Haber, Jeri Prante, and Jeff Ruskowitz for their encouragement and assistance throughout this entire process. Lastly, I would like to thank Dr. Keith Dennett and Dr. Glenn Miller for their service on my committee.

Table of Contents

List of Figures

List of Tables

Chapter 1 Introduction

Approaches to increased water demands in the 20th century relied on constructing dams and reservoirs to capture, store, and convey freshwater. These structures often have large economic and environmental implications and it is increasingly difficult to find sources of freshwater to meet ever growing needs of an increasing population (Gleick, 2000). In the past century, global populations have grown from 1.6 billion to over 7 billion, and arable land under irrigation has increased from 50 million hectares to 267 million hectares resulting in a 7-fold increase of freshwater withdrawal (Gleick, 2000). In the arid southwest region of the United States, up to half of all water demand goes towards the irrigation of public and private land. In this same region, certain climate models predict drought increases of 60 to 70% over the next century, necessitating the implementation of reclaimed and recycled water into public policy (Cayana et al., 2010).

The use of reclaimed water for non-potable uses has many benefits for both arid and wet climates. Recycling treated municipal sewage for irrigation and industrial uses reduces demand of potable water sources. This lowers the number of large dams and reservoirs which replace free running streams and rivers, saving money and limiting environmental impacts. In communities that require groundwater aquifers for potable water sources, the severity of water table reduction can be limited (Bruvold et al., 1981). Surface and groundwater discharge requirements are becoming ever more stringent, and the implementation of new regulations is increasingly expensive. Due to the lower water quality standards of reclaimed municipal wastewater, the costs associated with treating wastewater to surface and groundwater discharge standards can be reduced through the incorporation of reclaimed water into the municipal treatment regimen (Bouwer, 2002).

Water reuse is not without problems in implementation and public perception. Pathogens and viruses present potential threats to public health if the reclaimed water is applied to crops which are transported or consumed raw, though environmental pressures and disinfection of wastewater effluents act to mitigate the effects of pathogenic microorganisms. Reclaimed water typically has higher salinity levels than potable sources and it is difficult to remove dissolved solids without expensive membranes or cationic exchange resins. Increased salinity has negative effects on landscape and crop growth and may require operational control such as periodic irrigation with less saline water sources (Toze, 2005). High suspended solids and nutrient concentrations in reclaimed water sources can result in decreased soil hydraulic conductivity through direct clogging and growth of soil microorganisms.

Public perception is often mixed when reclaimed water is implemented into municipal policy and apprehension grows as the chance of contact increases. The potential for rising water demand and scarcity requires better reclaimed water quality and public education to meet the growing water needs in the 21st century (Toze, 2005).

The South Truckee Meadows Water Reclamation Facility and Huffaker Hills Reservoir supply the south Reno, NV, community with non potable irrigation water. The current study seeks to provide insight into the quality of reclaimed water provided to customers as well as necessary changes in treatment operation to obtain high end user satisfaction.

Chapter 2 Literature Review

2.1 What is an Oxidation Ditch?

Oxidation ditches are closed loop shallow ditches where biological carbon oxidation, nitrificiation, and denitrification occur. They are used primarily in small communities and residential developments. Oxidation ditches are beneficial due to their relatively stable effluent quality without intensive operator control (Goronszy, 1979). An aerial view and a schematic of the treatment processes of the oxidation ditch located at STMWRF is presented in Figures 2-1 and 2-2. Sewage influent first enters the end of the anoxic region where initial biochemical oxidation demand (BOD) removal and denitrification occurs. The mixed liquor next enters an aerobic region of the oxidation ditch where the rest of BOD is removed, and nitrification and phosphorus accumulation occurs. Oxygen levels are maintained by a fine-bubble aeration system. Finally, the mixed liquor flows through the anoxic region where nitrites (NO_2^-) and nitrates (NO_3^-) undergo denitrification and mixed liquor effluent is discharged.

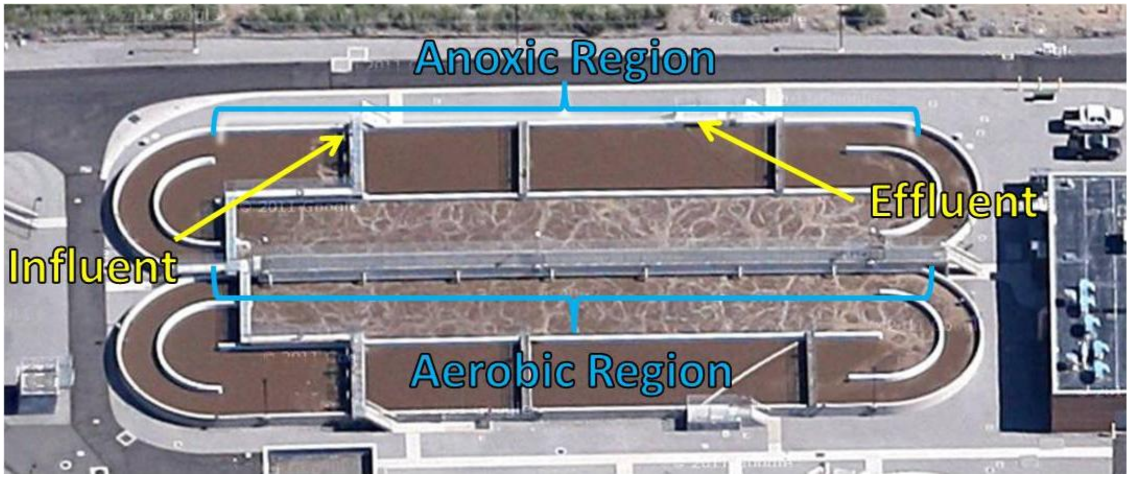

Figure 2-1: Aerial View of Oxidation Ditch at STMWRF

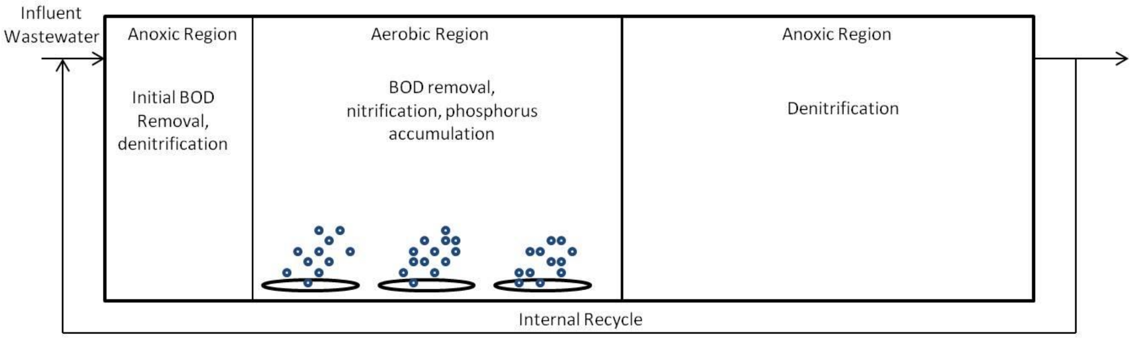

Figure 2-2: Schematic of Oxidation Ditch Treatment Process

Due to the eutrophication potential of nutrients in wastewater, primarily phosphorus and nitrogen, it is important that they are removed prior to discharge into receiving waters. Phosphorus removal is achieved in aerobic biological processes through uptake and assimilation into biomass (Insel et al., 2005). The stoichiometric formula for biomass is $C_5H_7O_2NP_{0.1}$ with phosphorus accounting for 2.7% of the dry cell weight. Effluent concentrations of phosphorus tend to decrease as solids retention time (SRT) decreases and BOD removal increases (Rittmann and McCarty, 2001). If effluent phosphorus concentrations are too high, enhanced biological phosphorus removal (EBPR) may be necessary. In order to achieve EBPR, influent water must first enter an anaerobic region where BOD oxidation is insignificant. In anaerobic regions, facultative anaerobic bacteria convert many organic compounds into fermentation products, primarily acetate, which is necessary for adenosine triphosphate (ATP) production by aerobic bacteria. The uptake of fermentation products is achieved by using stored poly-P as an energy source which is released as orthophosphate. Mixed liquor in the anaerobic region next flows into an aerated zone where production of ATP and poly-P occurs. Biomass from EBPR can attain 2 to 5 times the phosphorus content of normal biomass (Rittmann and McCarty, 2001). Despite the release of orthophosphate in the anaerobic region, the orthophosphate demand in the aerobic region is higher due to bacterial growth and the formation of ATP and poly-P results in lower effluent phosphorus concentrations (Romanski et al., 1997). Although EBPR is not intentionally incorporated in STMWRF's oxidation ditch, on-off cycles of aeration may lead to extended and cyclical anaerobic/aerobic periods which may facilitate EBPR.

As stated above, nitrogen has the potential to cause eutrophication in receiving waters and must be removed prior to discharge. Nitrogen removal is achieved in oxidation ditches through nitrification and denitrification. Nitrification occurs through the oxidation of ammonium (NH_4^+) to nitrate by obligate aerobes in aerobic regions. The stoichiometric formula for the oxidation of ammonium is:

$$- \quad - \quad ^{-} \quad - \qquad (1)$$

Ammonium is first converted to nitrite by ammonium-oxidizing nitrifiers followed by nitrite oxidation to nitrate by nitrite-oxidizing nitrifiers. As obligate aerobes, nitrifiers do not function well in low DO environments where many heterotrophs thrive and are comparatively slow growers due to the low energy yield of nitrogen electron donors (Rittmann and McCarty, 2001).

Denitrification, on the other hand, is accomplished by facultative aerobes which switch to nitrite or nitrate respiration when O_2 is limited in anoxic environments. The reduction of NO_x to N_2 gas is a sequence of steps facilitated by enzymatic catalysts. The half reaction of denitrification is:

$$^{-} \qquad (2)$$

Although denitrification occurs primarily in anoxic environments, low oxygen concentrations less than 2.5 mg O_2/L still permit denitrification in small quantities (Rittmann and McCarty, 2001) .

Oxidation ditches are often subject to diurnal influent loads due to a lack of flow control structures. Assuming constant aeration intensity and variations in influent loading, fluctuations in dissolved oxygen are inevitable. Insufficient aeration and over-aeration may cause temporal instabilities in nutrient removal (Insel et al., 2005).

2.2 Microorganism and Algae Dynamics in Wastewater Effluent Reservoirs

The growth rates and photosynthetic activity of algae are dependent on the light intensity in the water column. Light intensity is often measured in units of foot-candles (ft-c). One ft-c is equivalent to the light intensity of a standard candle at a distance of one foot while 1,000 ft-c is equivalent to the light intensity of 1,000 standard candles at a distance of one foot. For various green algae, growth rates increase as light intensity increases, and growth plateaus are reached between 250 to 500 ft-c at $25^{o}C$ depending on the type of algae. Inhibition can occur between 600 to 2,000 ft-c at $25^{o}C$ where growth rates decline below the maximum value. As temperatures increase, green algae are capable of maximum growth rates at higher light intensities (Sorokin and Krauss, 1956). Typical light intensities at the earth’s surface are 1,000 ft-c during overcast weather and 10,000 ft-c with unobstructed direct sunlight. Various atmospheric factors affect light intensity on the earth’s surface such as suspended particulate matter and humidity, while turbidity, such as suspended particles and microorganisms, decrease light intensity within the water column (Ryther, 1956).

As algae grow and photosynthetic activity increases, pH levels increase due to the consumption of inorganic carbon and DO increases due to the release of oxygen (Chen and Durbin, 1994). A study conducted by Oswald et al. (1957) examined the BOD removal efficiencies of algae grown in wastewater stabilization ponds. The researchers found that for algae concentrations greater than 100 mg/L dry weight, DO was consistently greater than 15 mg O_2/L and as high as 22 mg O_2/L in July and August. In addition, pH reached levels near 11 during times of vigorous algae growth. Another study conducted in Ames, Iowa, by Raschke (1970) consisted of a series of wastewater stabilization ponds which sought to determine treatment procedures that would produce high quality effluent. The DO ranged from 13.2-32.6 mg O_2/L while pH levels fluctuated between 8.5 and 9 throughout the summer. The DO and pH levels found in the previous studies are greater than the oxygen saturation limit and at the upper reaches of the pH range of natural waters. The elevated levels are suspected to be the cause of highly active algae growth and photosynthesis.

Algal growth and activity are also affected by the nutrient composition of their environment. Nitrogen and phosphorus are the two most critical non-carbon nutrients for algal growth, and the N:P ratio is used to determine which nutrient limits different strains of algae. The ideal N:P ratio for a particular strain of algae occurs during the transition from one limiting nutrient to the other. There are wide variations in the N:P ratio depending on the particular species, with an overall range from 7 to 25. Most algae have an ideal N:P ratio between 7 and 15 and thrive in environments with nitrogen and phosphorus concentrations that are similar to their ideal N:P ratio (Rhee and Gotha, 1980).

Orthophosphate is the most critical phosphorus nutrient and typically limits algal growth in most natural waters. It is involved in the Calvin-Benson cycle, which leads to the reduction of CO_2 during photosynthesis. Phosphorus-deficient algae are photosynthetically and photoreductively inhibited, which is most pronounced in light-saturated conditions (Kessler et al., 1957). Raschke (1970) found that during the period of highest algae productivity in the wastewater stabilization ponds (July and August), orthophosphate concentrations were reduced by 11-88% and attained a minimum concentration of 1.1 mg P/L.

Nitrogen is necessary for the production of amino acids and the production of biomass in plants and algae. While algae are capable of assimilating many forms of nitrogen, ammonia-assimilating algae grow faster in all light intensities compared to algae which assimilate nitrate, nitrite, and dinitrogen. Nitrate assimilation is inhibited in environments with ammonia concentrations exceeding 10^{-5} M (0.14 mg N/L) (Paasche, 1971). Raschke (1970) found in the previously described wastewater stabilization ponds that NH_4^+ reductions of 41-100% were achieved in July and August during the highest periods of algae productivity.

Algae that grow in nitrogen starved environments experience long-term negative effects related to photosynthesis, nitrogen uptake, and growth. Organic matter deficient in nitrogen (e.g., carbohydrates and fats) is synthesized rapidly while organic matter high in nitrogen (e.g., chlorophyll and amino acids) is degraded. Nitrogen starvation reduces photosynthetic enzymes involved in the Calvin cycle while enzymes responsible for nitrogen synthesis are increased dramatically. In ammonia-assimilating algae, nitrate reductase enzymes increase substantially after 10 hours of nitrogen starvation, allowing the algae to uptake a variety of nitrogen forms (Hipkin and Syrett, 1977). In environments with sufficient nitrogen, unionized ammonia (NH_3) can be toxic to algae when present at concentrations exceeding 2 mM (28 mg N/L) and pH levels greater than 8. Ammonia toxicity arises from its ability to cross cell membranes due to its neutral charge. As ammonia diffuses into the cell, the internal pH of the cell can increase to inhibitory levels and cause a reduction in photosynthetic activity (Abeliovich and Azov, 1976).

Algae are capable of utilizing various forms of inorganic carbon for use in biomass. Carbon dioxide has been found to be the dominant form utilized by most algae, though bicarbonate is also favorable. As pH increases, dissolved concentrations of CO_2 decrease and can become limiting as bicarbonate concentrations increase. Decreased levels of carbon uptake have been observed at pH levels around 8, and it is suspected that this is caused by low levels of dissolved CO_2 (Chen and Durbin, 1994). Basic environments with pH levels around 9 inhibit photosynthesis and growth due to the reduced solubility of transition trace metal nutrients such as iron, the inhibition of enzymatic uptake of essential nutrients, and increased concentrations of carbonate and hydroxide ions which induce toxic effects to the organism as well as cause direct cellular and enzymatic damage (Moss, 1973).

The symbiotic and inhibitory relationship of algae and bacteria determines the growth capabilities of both kinds of microorganisms. Bacteria can aid in the stimulation of algal growth through the remineralization of nutrients and the production of vitamins in environments where nutrients are limited. On the other hand, algae provide nutrients (e.g., nitrogen) and energy sources (e.g., organic carbon, dissolved oxygen) through decomposition and photosynthesis that aid in bacterial growth. The cohabitation of algae and bacteria can also cause growth inhibition between the microorganisms. Active algal activity can inhibit the growth of microorganisms if pH increases associated with photosynthesis reach levels that inhibit both bacterial and algal growth. Bacteria can inhibit algal growth through respiration at night where decreases in O_2 concentrations may create anaerobic environments that inhibit photosynthesis. Because bacteria are in competition with algae and are generally better at assimilating nutrients, algal growth is less successful in environments where bacterial activity is high and nutrient availability is low (Cole, 1982).

2.3 Effects of Filtration and Chemical Coagulation on Effluent Algae Concentrations

Individual algae cells are small in diameter and are often less than 0.45 μm in size. Media used to filter algae, such as sand, has to have a grain size less than 0.335 mm for effective removal when chemicals are not added (Naghavi and Malone, 1986). Due to the negative surface charge and specific gravity (less than 1.0) of the cell, algae do not easily settle out of suspension without chemical addition. Coagulation is based off of DLVO theory (named after

Derjaguin, Landau, Verwey, and Overbeek), which states that coagulation is a balance between attractive Van der Waals forces and the electrical repulsion between particles. Repulsion can be altered by changing the ionic strength of the suspending medium in order to modify the particle surface charge, allowing particles to come into close proximity to each other so that Van der Waals attraction can predominate. When Fe(III) and Al (III) salts are added to water, the following hydrolysis reactions occur:

(3)

(4)

In order to attain charge neutralization of algae cells, positively charged metal-hydroxides must predominate in solution. This occurs at pH levels below the isoelectric point of alum (pH < 8) and ferric chloride (pH <7).

Algae flocculation is thought to be attributed to charge neutralization combined with precipitate formation (Wyatt et al., 2011). As coagulant dosage increases, the floc density reaches a point where precipitates begin to interact with one another and form larger flocs. As the large flocs are formed they enmesh suspended algae and remove them as they settle. This is known as sweep flocculation and marks the transition from removal dominated by charge neutralization and bridging to flocs sweeping suspended algae out of solution. At high algae concentrations, the minimum amount of coagulant required to attain high flocculation efficiency becomes independent of algae concentrations as the removal mechanism switches from charge neutralization to sweep flocculation (Wyatt et al., 2011).

Many studies have been conducted in which alum and ferric chloride were used as coagulants for the removal and harvesting of algae. A study conducted by Golueke et al. (1965) examined the feasibility of harvesting and processing sewage-grown algae through chemical coagulation and sedimentation. The researchers reported that 99% of algae cells were removed at an alum dose of 75 mg/L and a pH level of 6.3. In another study conducted by Friedman et al. (1977), alum was used to coagulate algae in order to determine the effects of varying algae concentrations on alum requirements. The researchers reported 90% removal of algae at concentrations of 50, 100, and 200 mg/L dry weight with alum concentrations of 45, 90, and 180 mg/L, respectively. Experiments were carried out in solutions with initial pH levels of 7.5. Wyatt et al. (2011) found that ferric chloride efficiency was dependent on algal density when algae concentrations were low. The researchers found that for removal efficiencies greater than 90%, a linear relationship existed between required ferric chloride dose and algae concentration. They reported 90% removal at initial algae concentrations of 50, 100, and 200 mg/L dry weight with ferric chloride doses of 90, 125, and 170 mg/L, respectively. However, at algae concentrations greater than 500 mg/L dry weight, they discovered that the number of charged iron species per algae cell to attain high flocculation efficiency decreased in a power law fashion due to the change from charge neutralization to a sweep floc removal mechanism. Van Vuuren and Van Vuuren (1965) found that concentrations of ferric chloride and alum in excess of 100 mg/L are often necessary to achieve removal greater than 90% of algae grown sewage maturation ponds.

Studies have been conducted in which influent to a coagulating chamber is first oxidized to aid in algae removal. Preoxidation is thought to aid in coagulation by destabilizing the negative charge on algae cell surfaces. Chen et al. (2009) found that algae removal efficiencies increased by 10% when preoxidation was coupled with alum coagulation. The researchers determined that 1.2 mg O_3/L was the optimal preoxidant dose for increasing algae removal efficiencies at alum doses ranging from 10 to 40 mg/L. The researchers also found that high preoxidant doses had an inhibitory effect on coagulation due to cell lysis, which releases organic matter into solution that competes for coagulant.

2.4 Reclaimed Water Distribution Systems

Reclaimed water can be beneficial as a water source due to the increased nutrient concentration compared to potable water sources. Fertilization requirements are often reduced when landscapes undergo a change from potable to reclaimed water irrigation (Devitt et al., 2005). Excessive nutrients can cause problems to plants as nitrogen and phosphorus levels in wastewater are often greater than plant demands. Excessive growth, uneven maturity, and reduced quality are often byproducts of over fertilization from reclaimed water sources (Asano, 1987).

Reclaimed water stored in open-air reservoirs often contains high concentrations of algae. Algae increase disinfectant demand and turbidity when organic carbon is released through enzymatic processes and cell decay. Bacteria use the organic carbon as a food source and decrease the disinfectant residual further down the distribution system. In closed tank reservoirs, disinfection concentrations can reach low levels that allow for bacterial growth and anaerobic conditions. However, excessive disinfection to combat these issues may inhibit plant growth. Chlorine concentrations less than 1 mg Cl_2/L should not affect foliage while concentrations greater than 5 mg Cl_2/L can lead to severe damage (Jjemba et al., 2010).

Chapter 3 Research Goals

Currently, the quality of Washoe County reclaimed water has experienced challenges in meeting the standards that end users demand, in part, due to filter clogging and water color associated with algae growth. The primary objective of this study was to determine how the storage reservoir water quality changed throughout the distribution season, as well as operations at the reclamation facility that could affect the water quality delivered to customers. The main objective was to monitor algae growth in the Huffaker Hills Reservoir and nutrient degradation throughout the distribution season. Secondary goals were to determine how current operations at STMWRF affected nutrient loading into the reservoir, and the potential for chemical coagulation to decrease the turbidity of distribution system influent. This was accomplished through jar tests and pilot-scale filtration tests where alum and $FeCl_3$ were used as coagulants. The results from these research studies have been used to make recommendations to increase end user water quality.

Chapter 4 Methods and Materials

4.1 Oxidation Ditch Efficiency

4.1.1 Oxidation Ditch Efficiency Experimental Setup

An aerial view of the South Truckee Meadows Water Reclamation Facility (STMWRF) is presented in Figure 4-1 showing where oxidation ditch influent and effluent samples were collected. Influent sample water was collected at the headworks just after the bar screens. Effluent sample water was collected at the MLSS distribution structure just prior to the secondary clarifiers. Samples were collected every hour over a 24 hour period using a Teledyne Isco 3700 full-size portable sampler (Lincoln, NE). A peristaltic pump distributed 100 mL grab samples through 3/8 inch vinyl intake tubing into one liter glass bottles. The glass collection bottles were spiked with 0.5 mL of concentrated mercuric chloride (50 mg $HgCl_2$/L) and surrounded with ice prior to collection in order to inhibit microbial activity and nutrient consumption during the 24-hour sampling process.

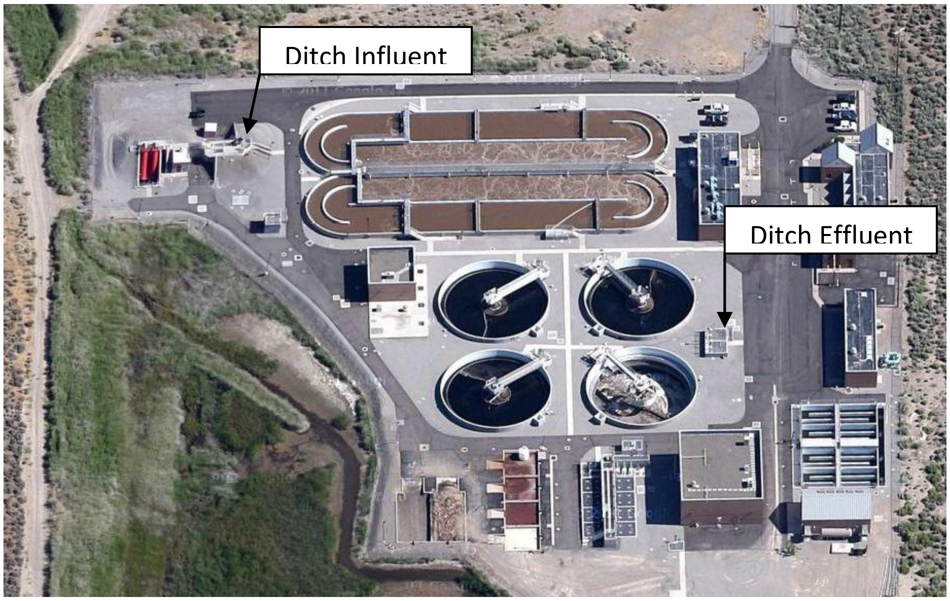

Figure 4-1: Location of Oxidation Ditch Influent and Effluent Sample Collection Points (Google, 2012)

4.1.2 Plant Flow and Dissolved Oxygen Measurements

Continuous measurements of plant information are controlled and compiled by Supervisory Control and Data Acquisition (SCADA) system. Influent plant flow was recorded every 12 minutes from SCADA and an hourly flow value was determined by averaging five 12-minute flow values throughout an hour. For example, flow values from 4:36, 4:48, 5:00, 5:12, and 5:24 were averaged to determine the flow at 5:00. DO probes were located in the eastern edge of the oxidation ditch at the end of the aerated region. DO data were compiled from SCADA at the top of each hour during the sampling period. Random DO samples were taken using a YSI 556 DO probe to check the accuracy of SCADA measurements. Further explanation of YSI 556 multi-probe measurements will be discussed in Section 4.5.

4.2 Huffaker Hills Reservoir

4.2.1. Experimental Setup

Weekly water quality measurements were collected at Huffaker Hills Reservoir from April 26, 2011 to October 18, 2011. Samples were collected at three locations within the reservoir determined in consultation with engineers at the Washoe County Department of Water Resources and CH^2M Hill. Location A was at the northeast position of the reservoir and had a bottom elevation equal to the average of the entire reservoir. Location B was positioned above the intake and plant discharge pipe and the reservoir floor was at an elevation approximately four feet lower than Location A. Location C was positioned on a raised area just north of the dam with a reservoir floor elevation approximately 15 feet higher than Location A. An aerial view of the reservoir showing the three sampling locations is presented in Figure 4-2. Samples were collected using a 14 foot NRS River Cataraft (Moscow, ID) in five foot intervals from the reservoir surface using a WildCo Alpha horizontal water sampler (#1120-G42, Yulee, Fl) and water quality parameters (i.e., pH, temperature, conductivity, and ORP) were measured in the field using a YSI 556 multiprobe. Samples were stored in 500 mL plastic bottles and placed in an ice packed cooler. Nutrients (ammonia, orthophosphate, nitrate, total nitrogen) and turbidity were measured in the lab. A Sargent-Welch Secchi disk (#WL9719, Buffalo, NY) was used to assess water clarity.

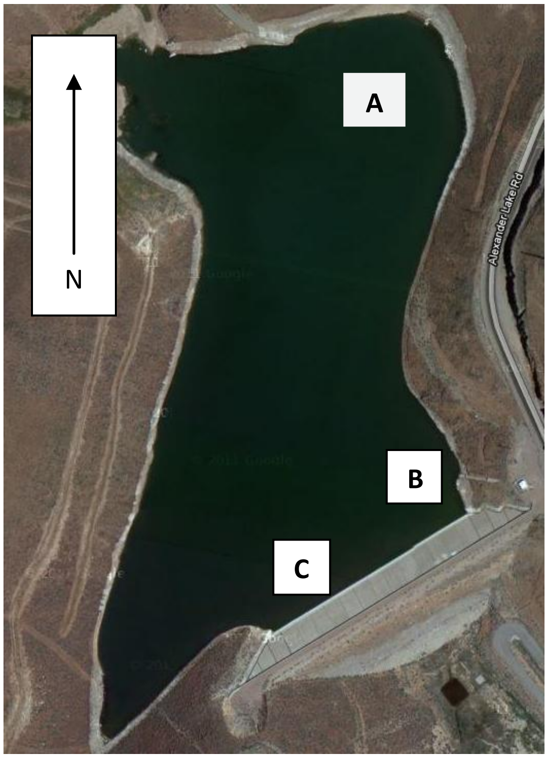

Figure 4-2: Sampling Locations at Huffaker Hills Reservoir (Google, 2012)

4.3 Washoe County Reclaimed Water Distribution System

Weekly water quality measurements were collected from various locations within the distribution system. Washoe County inspectors performed sample collection and water quality measurements (i.e., pH, temperature, conductivity, and ORP) in the distribution system at five locations (i.e., Trademark, Wilbur Mae, Damonte Ranch, Field Creek, Arrow Creek) presented in Figure 4-3. Samples were stored in 500 mL plastic bottles and kept in an ice cooler until laboratory analysis. Turbidity was measured every week and nutrient analyses (i.e., ammonia, orthophosphate, nitrate, and total nitrogen) were performed on a biweekly basis.

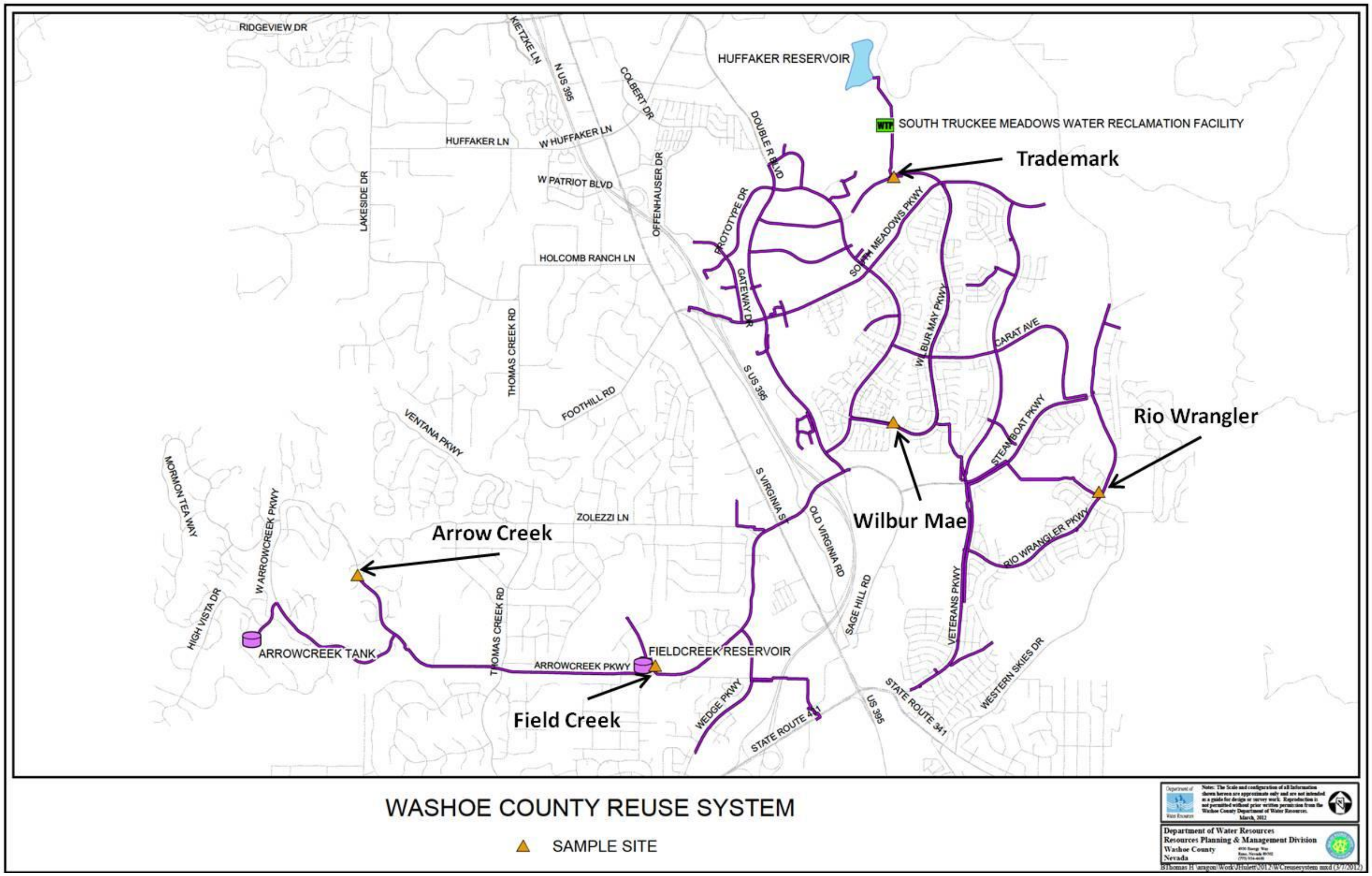

Notes: The Scale and configuration of all information shown hereon are approximate only and are not intended as a guide for design or survey work. Reproduction is not permitted without prior written permission from the Washoe County Department of Water Resources.
March, 2012

Department of Water Resources
Resources Planning & Management Division
Washoe County
Nevada

B\Thomas H \aragon\Work\JHulett\2012\WCreusesystem mxd (3/7/2012)

Figure 4-3: Washoe County Reclaimed Water Distribution System and Sampling Locations (Hulett, 2012)

4.4 Jar Tests and Filtration

4.4.1 Jar Test Experimental Setup

The purpose of this portion of the study was to evaluate the effects of ferric chloride ($FeCl_3$) and aluminum sulfate ($Al_2(SO_4)_3$) on turbidity removal from a mixture of reservoir and secondary clarifier effluent at STMWRF. Jar test studies were conducted on water collected the previous night from the filter influent channels. The sample water was initially tested for turbidity using a Hach 2100 N turbidimeter and pH using a YSI 556 multi probe. Six two-liter B-KER^2 square jars were filled with sample water and placed into a Phipps and Bird PB-700 jar test apparatus (Richmond, VA). The mixer was set to 100 rpm and coagulant was introduced into each jar at dosages of approximately 6, 18, 30, and 42 mg/L. The samples were mixed at 100 rpm for one minute to simulate rapid mixing then mixed at 15 rpm for five minutes to simulate flocculation. The mixer was then turned off and the samples were allowed to settle. Turbidity measurements were taken from each jar at two, eight, and twelve minutes after the mixer was turned off and pH measurements were taken between 2.5 and 5 minutes.

4.4.2 Filtration Experimental Setup

A pilot-scale filtration study was conducted to evaluate the effects of coagulation and filtration on turbidity removal of reservoir and secondary effluent. A schematic of the experimental configuration of the filter columns is presented in Figure 4-4. A submersible pump was used to collect water at night from the filter influent channels and the water was stored in a 200 gallon tank. A constant head tank was situated on top of the holding tank in order to deliver a constant water flow to the in-line static flash mixers with interior baffling and filter columns constructed of 6-inch diameter Lucite. A series of 90 degree elbows in the influent pipe reduced turbulent flow into the constant head tank. Two one-inch pipes directed water from the constant head tank to flash mixers where coagulant was added to one filter column. A 0.75-inch hose delivered the sample water to the filter columns. Flow through the flash mixers was controlled with 0.5-inch gate valves in order to maintain a constant coagulant dose. Coagulant was added to the sample water by a Watson-Marlow 520 series peristaltic pump (Wilmington, MA). The peristaltic pump flow was calibrated daily using a graduated cylinder and measuring the volume of coagulant pumped per rotation. The pump was then set digitally to deliver the desired coagulant dosage. The filter media consisted of two feet of gravel at the lower layer and two feet of sand as the upper layer. A 1.5-foot head was maintained in the column above the media surface of the sand bed to drive the filtration process and allow approximately two minutes of coagulation before filtration. This constant head level was maintained with three 0.5-inch ports connected to inline pumps. These ports and pumps were also used to dispose of backwash effluent. Flow through the filters was controlled with 0.5-inch gate valves which were calibrated daily to ensure a constant loading rate to the filters. The filter effluent flowed by gravity through a 0.75-inch hose and was collected into ten-gallon graduated buckets. A composite flow measurement was conducted over five-minute intervals during each filter run and effluent turbidity was measured every five minutes from the end of the hoses using the turbidimeter. Influent turbidity of the raw water was measured from the control filter influent hose. The duration of each filter run was 60 minutes. The filter columns were backwashed at the beginning and end of each filter run using No. 2 water at STMWRF. Each backwash cycle lasted for ten minutes during which the filter media bed was fluidized by approximately 100%. Following each backwash cycle the sand was agitated until it settled to a depth of 2 feet. The columns were treated with bleach weekly to control biofilm growth within the filter media which could contribute to head loss.

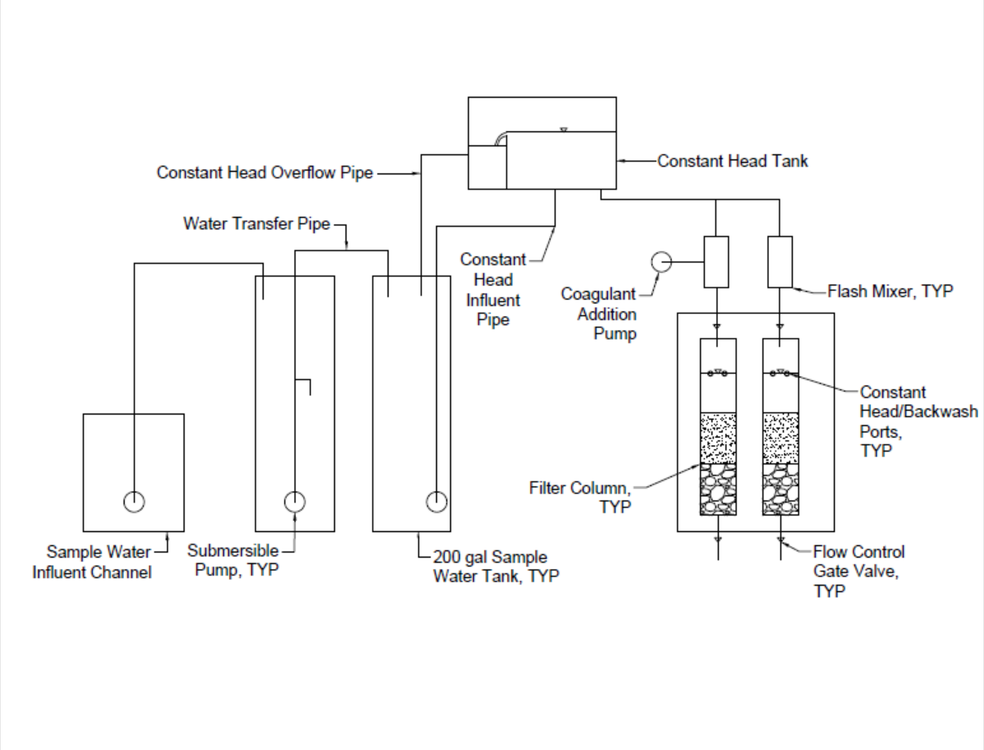

Figure 4-4: Pilot-Scale Filtration Schematic

4.5 Sample Analysis

4.5.1 Nutrients

4.5.1.1 Ammonia

Total ammonia, nitrate/nitrite, and orthophosphate analyses were performed on a Latchat Quikchem 8500 Automated Ion Analyzer (Lachat Instruments, Loveland, CO) using Quikchem methods 10-107-06-2-J, 10-107-04-01-A, and 10-115-01-1-V, respectively. The technique used to measure total ammonia is as follows: when ammonia is heated in the presence of salicylate and hypochlorite within an alkaline phosphate buffer, free ammonia is converted to monochloramine and an emerald green color is produced and monitored by a photodiode at 630 nm. Sodium nitroprusside is added to intensify the color. Photodiode voltage peak areas for known standards are measured and a calibration curve is developed relating time-integrated voltage to concentration. The voltage peak areas from the samples can then be compared to the calibration curve to determine the concentration. This method is appropriate for ammonia concentrations ranging from 0.30 to 30 mg N/L.

4.5.1.2 Nitrate/Nitrite

The technique for nitrate and nitrite is as follows: when nitrite diazontizes with sulfanilamide and couples with N-(1-napthyl)ethlyendiamine dihydrochloride, a water soluble magenta dye is produced which can be monitored at 520 nm. A copperized cadmium column was used to reduce nitrate to nitrite. When the column is included in the system, the measured concentration consists of only nitrite. Therefore, the nitrate concentration can be calculated by subtracting the “column off value” from the “column on value.” This method is appropriate for nitrite concentrations ranging from 0.2 to 20 mg N/L.

4.5.1.3 Orthophosphate

The technique for orthophosphate is as follows: when orthophosphate reacts with ammonium molybdate and antimony potassium tartrate under acidic conditions, a complex is formed and then that complex is reduced with ascorbic acid to form a blue complex which can be monitored at 880 nm. For both the nitrate/nitrite and orthophosphate methods, a calibration curve is developed in the same manner as for total ammonia.

For each method, a five point calibration curve was developed at the beginning of each run. Also, three check standards were included in each run, and as long as these check standards were measured within 10% of their actual value, the run was continued. Generally, the ammonia checks measured within 0-5% of their actual value. Orthophosphate and nitrate/nitrite checks were less accurate measuring within 2.5-10%.

4.5.1.4 Total Nitrogen

A Shimadzu Total Organic Carbon Analyzer (TOC-V_{csh}, Shimadzu Scientific Instruments, Kyoto, Japan) with an incorporated total nitrogen analyzer (Shimadzu TNM-1, Shimadzu Scientific Instruments, Columbia, MD) was used to measure total nitrogen by chemiluminescent detection. The combustion of nitrogen species at 720^{o}C over a platinum catalytic column produces nitrous oxide gas (NO). The nitrious oxide then interacts with ozone that is produced by an on-line generator and forms metastable nitrogen dioxide (NO_2). Nitrogen dioxide releases photons as it decays to ground state and these photons are measured by a photodetector and are proportional to total nitrogen concentration. As indicated by the instruction manual, a six point calibration curve was generated at the beginning of each run using potassium hydrogen phthalate ($KHC_8H_4O_4$), sodium bicarbonate ($NaHCO_3$), sodium carbonate (Na_2CO_3), and potassium nitrate (KNO_3).

Prior to nutrient analyses (i.e., ammonia, orthophosphate, nitrate, and total nitrogen), samples were syringe filtered through 0.20 µm CHROMAFIL Xtra PA-20/25 disposable syringe filters.

4.5.2 YSI 556 Multiprobe Measurements

The YSI 556 multiprobe (YSI Incorporated, Yellow Springs, OH) simultaneously measures pH, dissolved oxygen, conductivity, temperature, and ORP. Measurements are automatically corrected for temperature variations.

pH was determined using a glass combination electrode (#5565) that was frequently calibrated using buffer solutions of pH 4, 7, and 10. The pH probe measures in the range of 0-14 pH units with an accuracy of ± 0.2 pH units.

Dissolved oxygen was determined using a DO steady-state polarographic sensor with a 2 MIL PE membrane cap (#5909) that was frequently calibrated following the percent saturation method in Section 6.2.3 in the YSI 556 operations manual. The DO sensor measures in the range of 0 to 500% air saturation with an accuracy of ± 2%.

Temperature and conductivity was measured using a combined temperature/conductivity module (#5560) with a thermistor temperature sensor and 4 electrode cell conductivity sensor. Conductivity was calibrated frequently following the specific conductance method in Section 6.2.2 in the YSI 556 operations manual. The temperature sensor measures in the range of -5 to +45 ^{o}C with an accuracy of ± 0.15 ^{o}C. The conductivity sensor measures in the range of 0 to 100 mS/cm with an accuracy of ± 0.5% of the reading.

4.5.3 Turbidity

Turbidity was determined using a Hach 2100N turbidimeter (#4700000, Hach Company, Loveland, CO) which was frequently calibrated using standards of <0.1, 20, 200, 1,000, and 4,000 NTU.

4.5.4 Statistical Analyses

Descriptive statistical analyses of data (i.e., mean, standard deviation, box plots, confidence intervals) were performed using Microsoft Excel 2007 software. Analysis of confidence intervals was performed using a 95% interval of the data.

Chapter 5 Results and Discussion

5.1 Oxidation Ditch Removal Efficiency

5.1.1 Oxidation Ditch Influent Composition

The influent plant water was composed of untreated municipal wastewater. A typical nutrient composition of municipal wastewater is presented in Table 5-1, though it should be noted that different municipalities have varying concentrations of nutrients.

Table 5-1: Common Concentration of Municipal Wastewater Nutrients

Constituent	Concentration (mg/L)
PO_4^{-3}-P	5
NH_3-N	25
NO_3^--N	0.5

(Tchobanoglous et al., 2003)

The average nutrient composition of STMWRF influent is presented in Table 5-2. The nutrient concentrations in the influent were comparable to the average for municipal wastewaters cited in Table 5-1.

Table 5-2: Nutrient Concentrations of STMWRF Influent

Constituent	Average Concentration (mg/L)	Number of Observations
PO_4^{-3}-P	3.2 ± 0.7	n = 3
NH_3-N	21.5 ± 6.4	n = 3
NO_3^--N	0.5 ± 0.5	n = 3

The values given in Table 5-2 are average values throughout a 24-hour time period. Fluctuations occurred depending on the time of day and flow into the plant. Figure 5-1 shows the concentrations of ammonia and orthophosphate, plotted on the primary Y-axis, and flow, plotted on the secondary Y-axis, throughout the day. The error bars represent the standard deviation calculated from three days of sample data collected on February 1st, 5th, and 9th, 2012. Influent plant flow was highest in the morning and evening, corresponding to times when most of the local population is at home. During these times of high flow, concentrations of ammonia and orthophosphate were at peak levels. The lowest concentrations corresponded to the lowest flows which occured from midnight to 6:00 AM.

Municipal wastewater that does not contain agricultural runoff typically contains little nitrate (DNR, 2006). The average value of nitrate present in the STMWRF wastewater influent was 0.5 mg N/L. Although the average nitrate concentration was low, Figure 5-2 shows that the nitrate concentrations fluctuated throughout the day and the extent of the error bars show that nitrate concentrations fluctuated widely on a day to day basis. Nitrate concentrations followed the same trend as ammonia and orthophosphate, with the highest concentrations occurring in the morning and evening, and the lowest occurring at night.

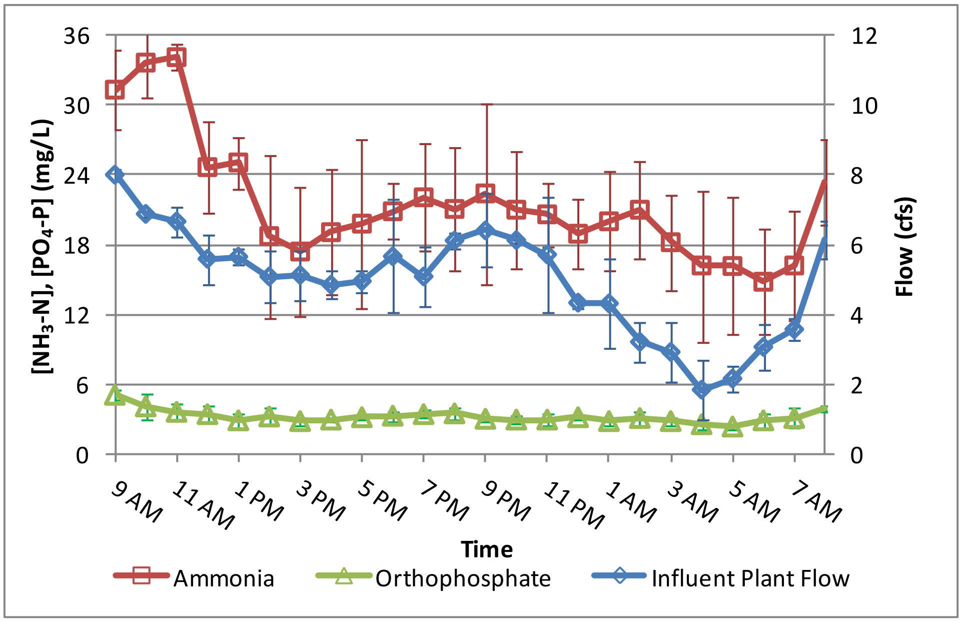

Figure 5-1: Average STMWRF Influent Nutrient Composition and Plant Flow

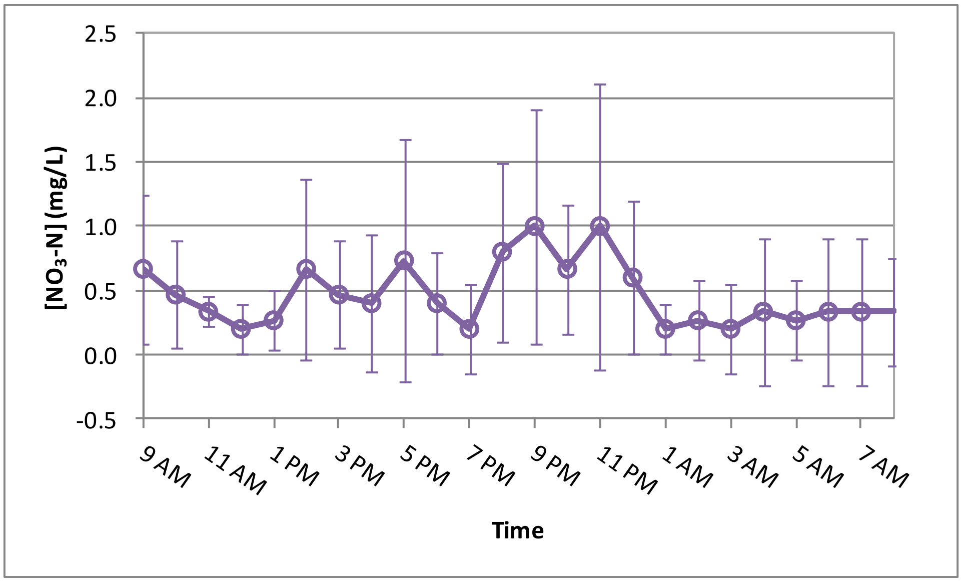

Figure 5-2: Average STMWRF Influent Nitrate Concentration

5.1.2 Oxidation Ditch Effluent Composition and Removal

5.1.2.1 Dissolved Oxygen

Plant influent enters an oxidation ditch which has both aerated zones and non-aerated zones. Due to fiscal concerns, the aeration blowers are not always operated to reduce power usage. Figure 5-3 shows the hourly average dissolved oxygen concentration collected from the SCADA system and concentrations measured manually using a YSI 556 DO probe. The probe that collected information for SCADA was not regularly calibrated. The YSI 556 DO probe was calibrated the morning each reading was taken and was likely more reliable. As can be seen in Figure 5-3, the YSI 556 DO probe readings were typically higher than the average values obtained from SCADA by 0.1 to 0.3 mg O_2/L.

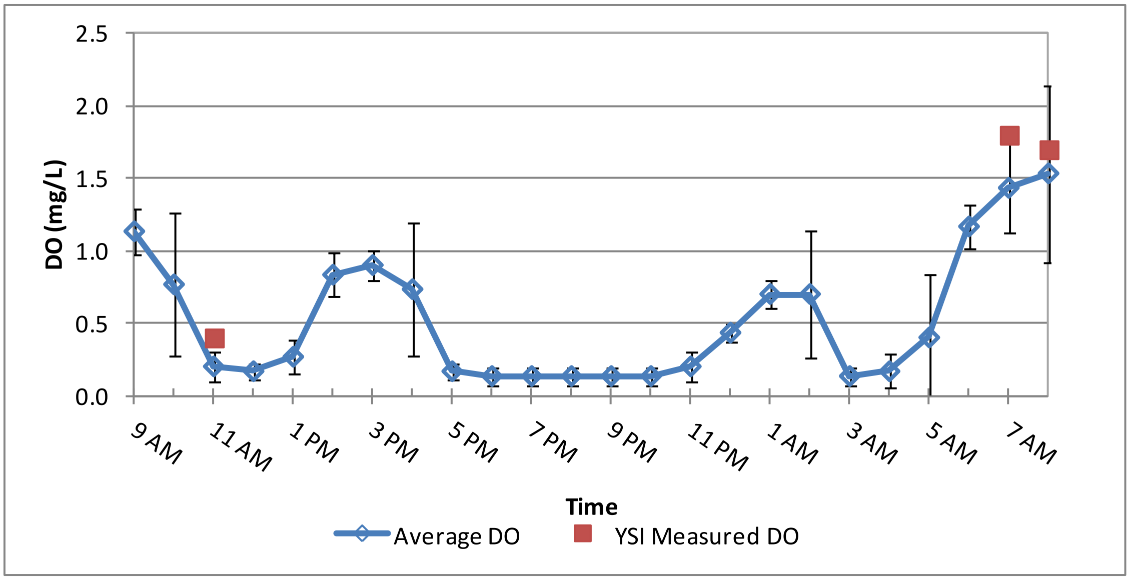

Figure 5-3: Dissolved Oxygen Concentrations in Oxidation Ditch Immediately after Aerated Region

Aeration in the oxidation ditch is turned off from approximately 11 AM to 1 PM, 4 PM to 11 PM, and 2 AM to 3 AM. This constitutes 11 hours in a day when aeration is not occurring. The lack of aeration can have significant effects on ammonia oxidation during nitrification due to low oxygen levels. Phosphorus removal is also affected by cyclical aeration in the oxidation ditch. As discussed in Section 2.1, EBPR may occur due to extended and cyclical anaerobic conditions.

5.1.2.2 Ammonia

5.1.2.2.1 Ammonia Concentrations and Removal

Ammonia is transformed in the oxidation ditch by nitrification, where nitrifying microorganisms use ammonia as an electron donor and oxygen as an electron acceptor, thereby producing nitrate. The hourly effluent concentrations of ammonia and DO from the oxidation ditch are presented in Figure 5-4. During periods of aeration (DO > 0.2 mg/L) ammonia concentrations decreased, and when the aeration time period was sufficient, ammonia concentrations reached levels which were typically less than 1 mg N/L. When aeration was stopped and DO concentrations decreased, ammonia levels increased and reached high levels greater than 6 mg N/L.

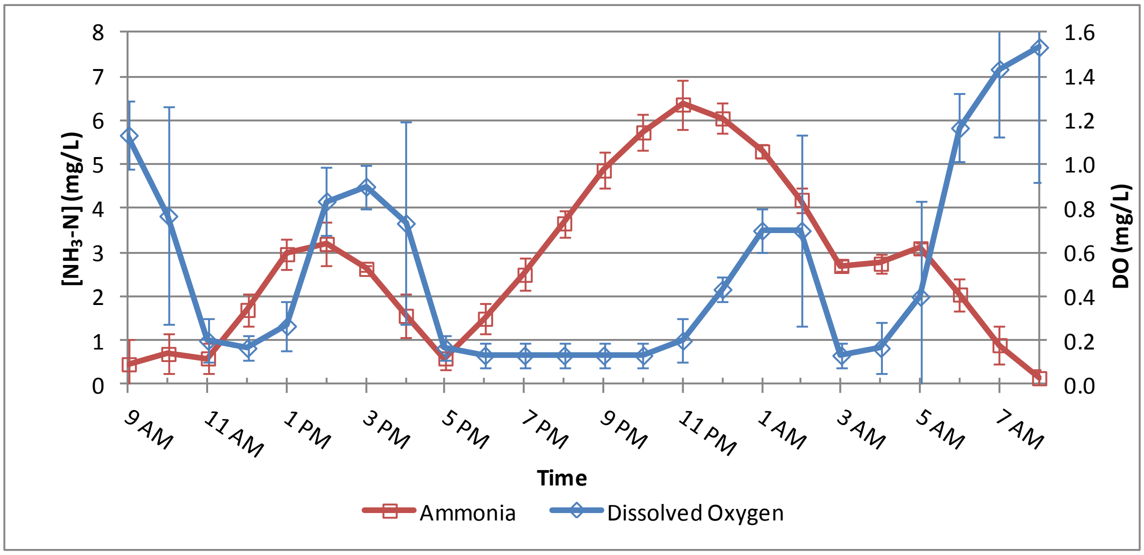

Figure 5-4: Hourly Effluent Ammonia and Oxidation Ditch Dissolved Oxygen

Since nitrification is the primary mode of ammonia conversion in the oxidation ditch, ammonia and nitrate concentrations should had an inverse relationship. Figure 5-5 presents the average ammonia and nitrate concentrations where error bars correspond to the standard deviation of the average from the three sampling days. When aeration was on, ammonia concentrations decreased to less than 1 mg N/L and nitrate concentrations increased to greater than 2 mg N/L. Conversely, when aeration was off, ammonia concentrations reached levels in excess of 6 mg N/L and nitrate concentrations were typically less than 0.5 mg N/L.

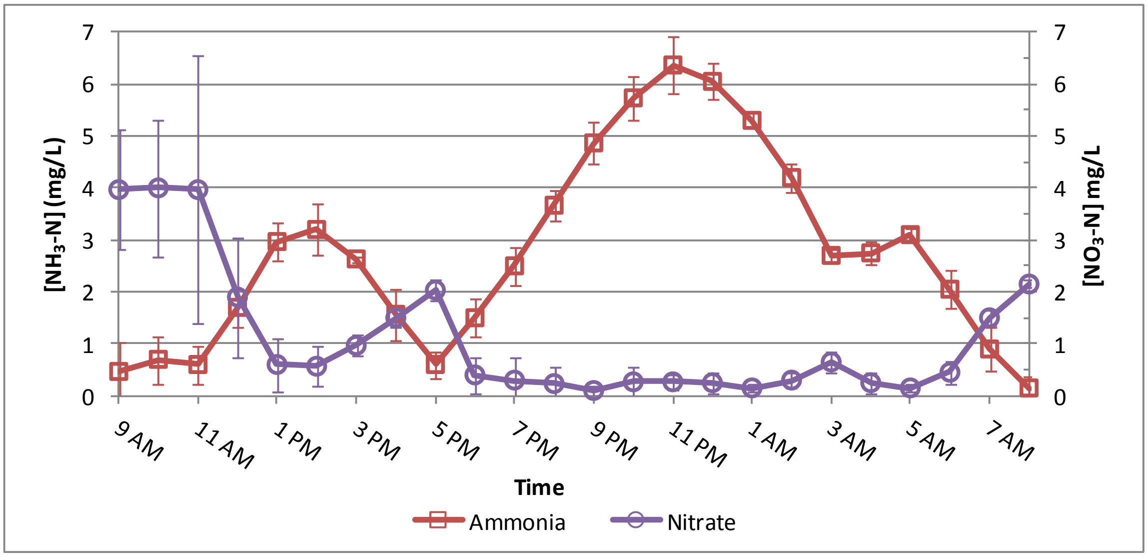

Figure 5-5: Average Ammonia and Nitrate Concentrations in Oxidation Ditch Effluent

5.1.2.2.2 Ammonia Release in Oxidation Ditch Effluent

The periodic high levels of ammonia present in oxidation ditch effluent could result in high levels of ammonia being released into Huffaker Hills reservoir if the high concentrations corresponded to times with high plant flow. In order to determine the mass of ammonia released, the hourly effluent concentrations of ammonia were multiplied by the hourly flow rates. Figure 5-6 presents the average mass of ammonia released per hour throughout the day based on influent flow rates from samples collected on Februray 1st, 5th, and 9th, 2012. During periods of extended aeration when ammonia concentrations were at the lowest levels (7 AM – 11 AM, 5 PM), the mass of ammonia released per hour was at a minimum (< 1 lb/hr). During periods of extended non-aerated conditions with elevated concentrations of ammonia, the majority of ammonia mass was released from the oxidation ditch.

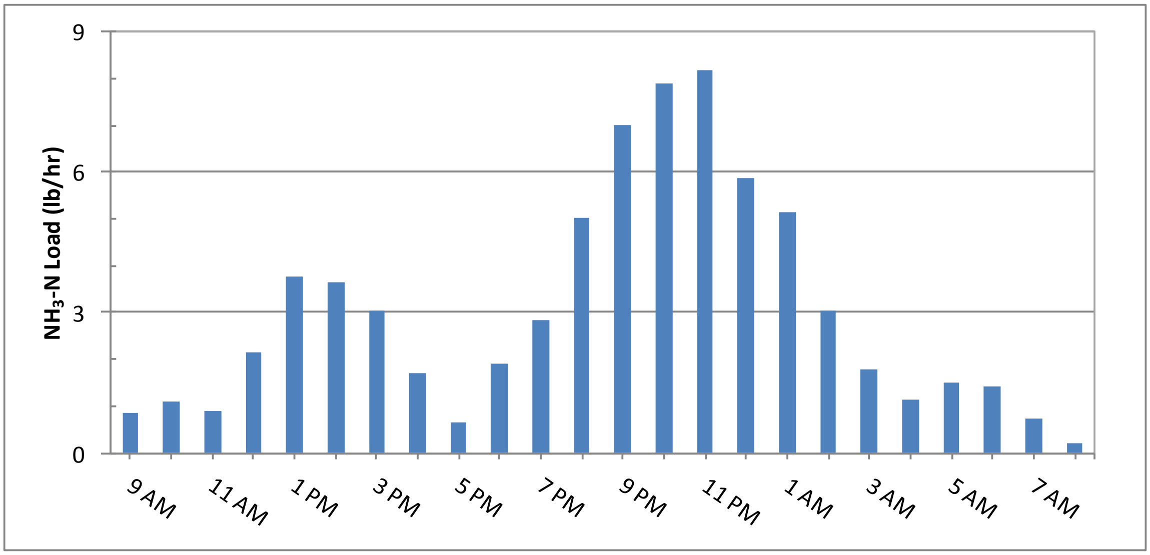

Figure 5-6: Average Ammonia Release in Oxidation Ditch Effluent

In order to determine the effects of infrequent aeration, the data were extrapolated to determine the mass of ammonia that would likely be released if aeration was continuous. An average ammonia concentration of 0.6 mg N/L was determined during the full aeration period when ammonia reached minimal levels. Ammonia concentrations from 12 PM to 4 PM and 6 PM to 6 AM were replaced with the average aerated value of 0.6 mg N/L. Using the influent flow values, the corrected, fully-aerated ammonia release was determined. Figure 5-7 presents the anticipated hourly ammonia released in a continuously aerated oxidation ditch. The mass of ammonia released daily from each scenario is compared in Table 5-3. By aerating the oxidation ditch continuously, the mass of ammonia released would be reduced by 78% compared to normal operation.

Table 5-3: Projected Ammonia Release in Oxidation Ditch Effluent

Scenario	Mass Released (lb NH_3-N/day)
Normal Operation	71.5
Continuous Aeration	15.7

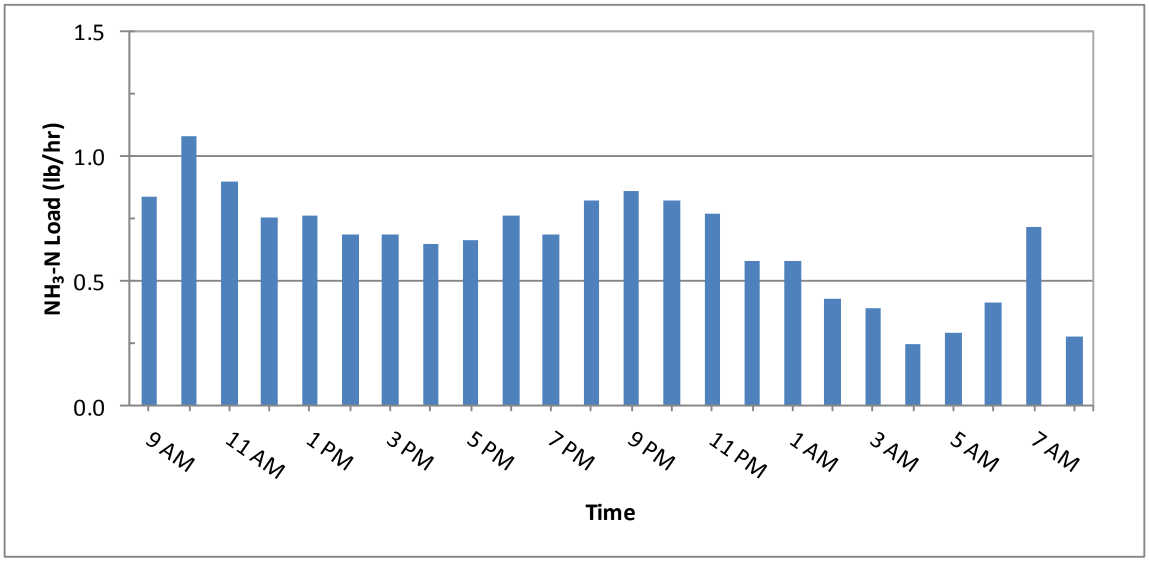

Figure 5-7: Average Ammonia Release from Continuously Aerated Oxidation Ditch Effluent

5.1.2.3 Orthophosphate

5.1.2.3.1 Orthophosphate Concentrations and Removal

As discussed in Section 2.1, anaerobic periods (represented by very low DO and nitrate concentrations) in oxidation ditches can lead to EBPR. Hourly concentrations of nitrate and DO are plotted in Figure 5-8. Error bars represent the standard deviation of data collected on February 1st, 5th, and 9th, 2012. From 6 PM to 11 PM, DO and nitrate concentrations were consistently less than 0.2 mg/L indicating that conditions in the oxidation ditch were anaerobic during this time. It is noteworthy that DO levels were measured in the upper region of the oxidation ditch, and lower levels likely had lower DO levels. The small range of the error bars for both nitrate and DO indicates that variations in concentration on a day-to-day basis were minimal. The consistent and cyclical periods of anaerobic conditions allow for the possibility of phosphorus accumulating organisms (PAOs) and EBPR in the oxidation ditch.

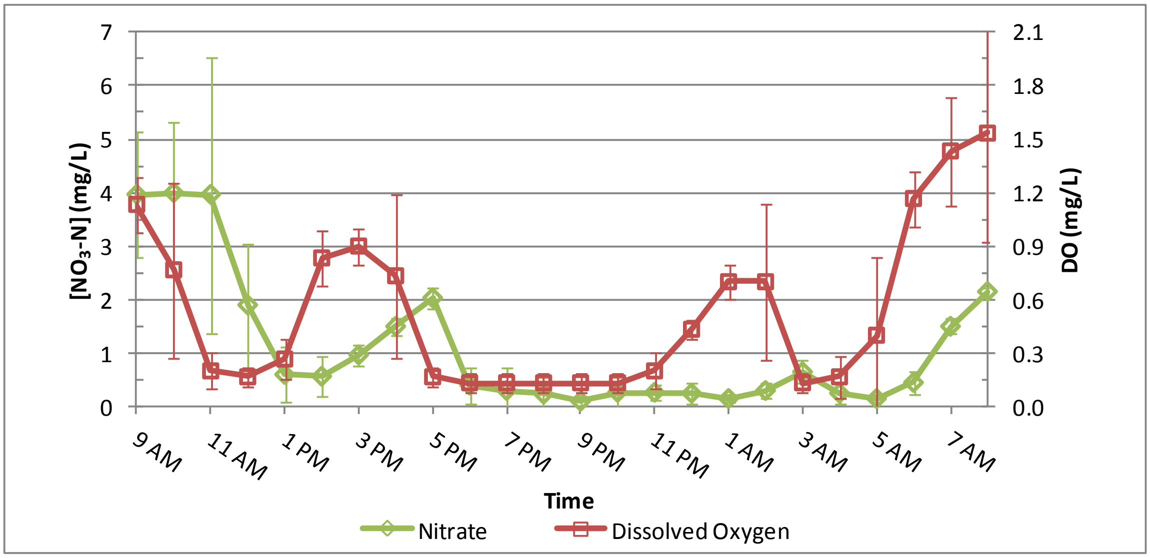

Figure 5-8: Effluent Nitrate and Oxidation Ditch Dissolved Oxygen

Figure 5-9 presents the average hourly phosphate concentration in the oxidation ditch effluent, plotted on the primary Y-axis, and the average hourly dissolved oxygen concentration plotted on the secondary Y-axis. Error bars represent the standard deviation from data collected on February 1st, 5th, and 9th, 2012. During extended periods of aeration, the concentration of orthophosphate is at a minimum (< 2 mg P/L). This is when PAOs would store phosphate as poly-P for anaerobic situations. During periods when the aeration system was off and DO and nitrate concentrations were low, orthophosphate concentrations reached levels in excess of 7 mg P/L. From Figure 5-1, the average orthophosphate influent concentration was less than 6 mg P/L and the average concentration was 3.2 mg P/L. This indicates that during extended anaerobic conditions, microorganisms released large concentrations of orthophosphate into the oxidation ditch which exceeded the maximum influent concentrations.

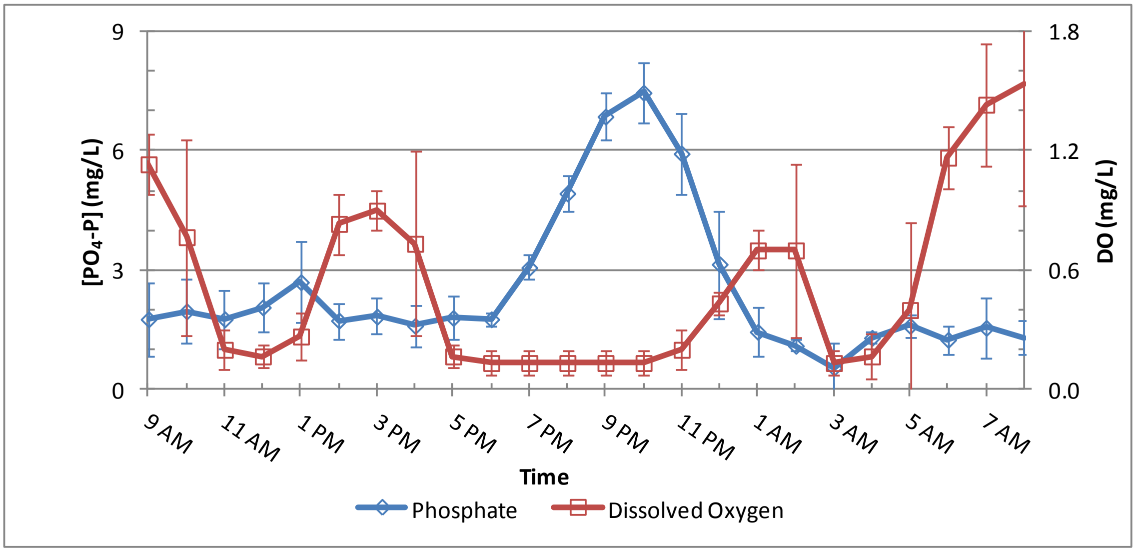

Figure 5-9: Effluent Orthophosphate Concentration and Oxidation Ditch Dissolved Oxygen Concentration

5.1.2.3.2 Orthophosphate Release in Oxidation Ditch Effluent

The periodic high concentrations of orthophosphate in the oxidation ditch effluent could elevate levels of orthophosphate in the Huffaker Hills Reservoir if high effluent concentrations correspond to high effluent flows. The hourly mass of orthophosphate released from the oxidation ditch was calculated in the same manner that ammonia was in Section 5.1.2.2.2. Figure 5-10 presents the mass of orthophosphate released per day based on oxidation ditch influent flows from data collected on February 1st, 5th, and 9th, 2012. During periods of extended aeration when orthophosphate was at the lowest concentrations (7 AM – 11 AM, 5 PM), the mass of orthophosphate released was at a minimum (< 3 lb P/hr). In the anaerobic period when aeration was off, the hourly mass released reaches high levels in excess of 10 lb P/hr.

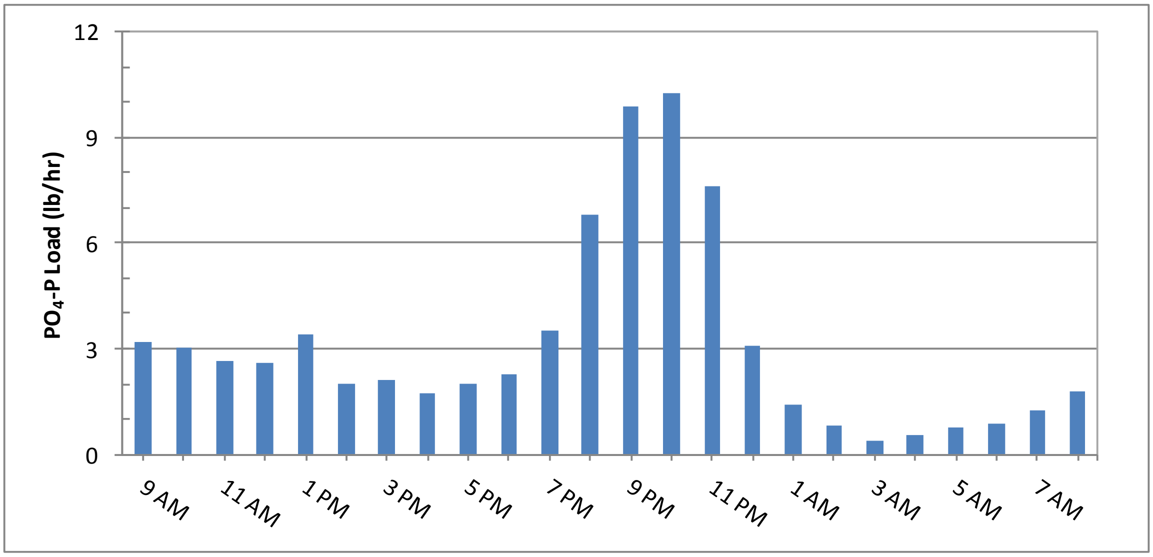

Figure 5-10: Mass of Orthophosphate Released in Oxidation Ditch Effluent

The orthophosphate concentration in the oxidation ditch effluent was extrapolated to determine the effects of cyclical aerobic periods on orthophosphate mass loading. An average concentration of orthophosphate during the extended aerobic periods was determined to be 1.6 mg P/L. This concentration was then applied to the high concentration time periods when aeration was off. Using influent flow values, the projected orthophosphate mass release for continuous aeration of the oxidation ditch is depicted in Figure 5-11. The mass of orthophosphate released daily from each scenario is compared in Table 5-4. Continuously aerating the oxidation ditch is projected to reduce the daily mass of orthophosphate released by approximately 40%.

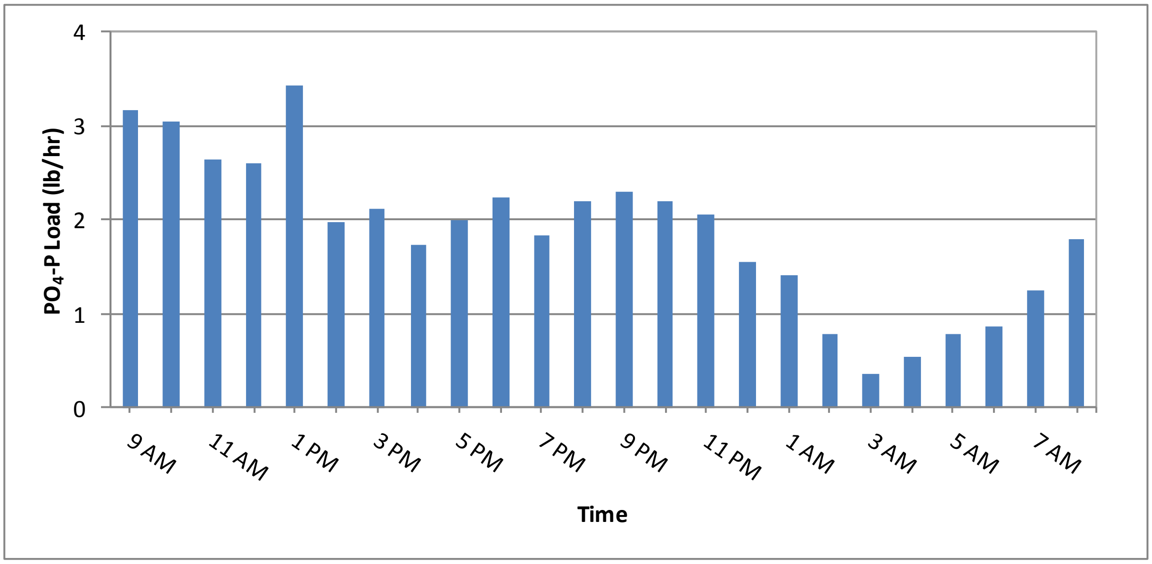

Figure 5-11: Mass of Orthophosphate Released in Oxidation Ditch Effluent Under Continuous Aeration

Table 5-4: Mass of Orthophosphate Released in Oxidation Ditch Effluent Under Continuous Aeration

Scenario	Mass Released (lb PO_4-P/day)
Normal Operation	73.9
Continuous Aeration	44.9

5.1.3 Disinfection of Oxidation Ditch Effluent

A free and combined chlorine concentration study was conducted on chlorine contact chamber effluent in order to determine the residual chlorine concentration as well as the effects of chlorination on ammonia concentrations. The reaction between ammonia and hypochlorous acid (HOCl) is extremely fast and has been reported to be 1.5×10^{10} M^{-1} h^{-1} (Harrington et al., 2003). Due to the fast second-order kinetic rate, it is hypothesized that residual concentrations of free chlorine, HOCl, suggest complete transformation of ammonia into chloramines. A summary of plant effluent chlorine concentrations is presented in Table 5-5. The first sample, collected at 9 AM on February 1st, was expected to have low ammonia concentrations (< 1 mg N/L) due to results presented in Section 5.1.2.2.1. Samples collected at 11:30 AM and 12:30 PM were expected to have higher concentrations of ammonia (> 1.5 mg N/L) due to results presented in Section 5.1.2.2.1. The sample collected at 9 AM had higher concentrations of free chlorine, and lower concentrations of chloramines due to the lower ammonia concentration. It is possible that free chlorine and chloramines present in plant effluent would persist in the reservoir, providing a residual disinfectant to inhibit biological growth. This will be discussed in further detail in Section 5.2.4.

Table 5-5: Disinfectant Concentrations from Chlorine Contact Chamber Effluent

Sample Collection Time	Free Chlorine (mg Cl_2/L)	Chloramines (mg Cl_2/L)
9:00 AM	1.0	1.2
11:30 AM	0.6	2.5
12:30 PM	0.7	2.4

5.2 Huffaker Hills Water Quality

5.2.1 Reservoir Water Temperature

The temperature of the reservoir water was measured using the YSI 556 multiprobe in five foot intervals from the surface. Figures 5-12 and 5-13 present the temperature profiles for seven sampling days taken at the beginning of each month for Location A and B, respectively.

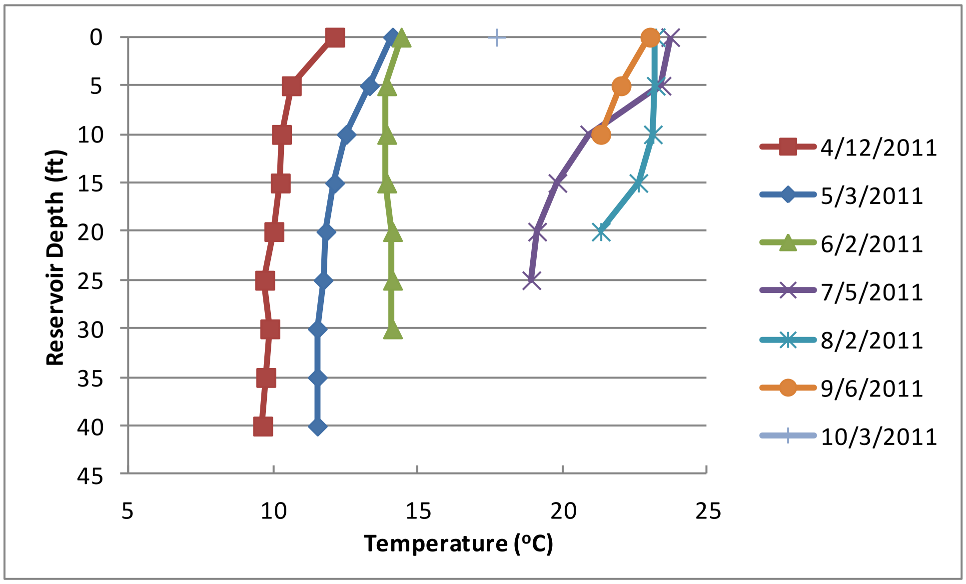

Figure 5-12: Temperature Profile at Reservoir Location A

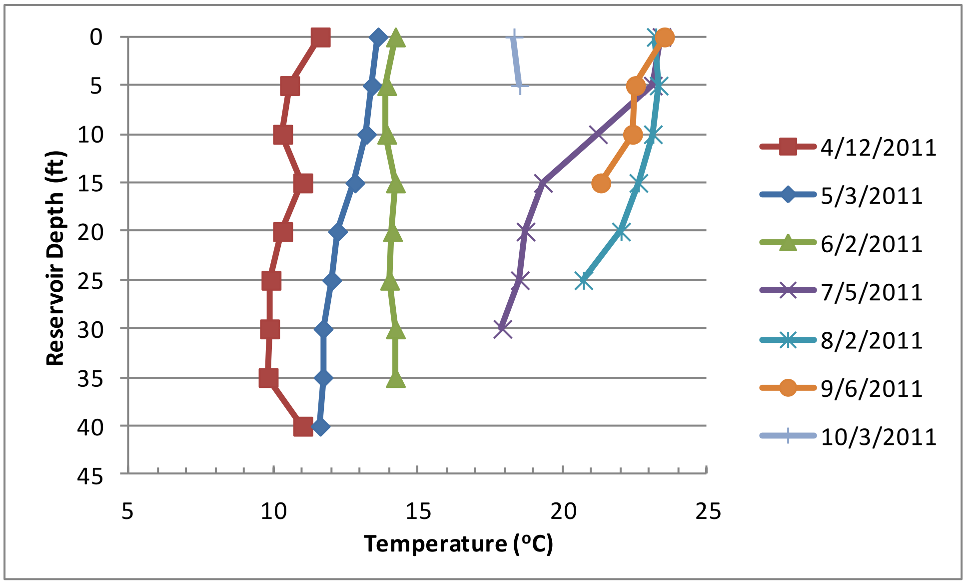

Figure 5-13: Temperature Profile at Reservoir Location B

From April to July, the temperature throughout the reservoir profile increased with the warmest temperatures existing at the surface. Temperatures were largely uniform from April to June at depths greater than five feet. In July, surface temperatures were warmer than deeper temperatures (by approximately 5 °C), with a clear thermocline existing around 10 feet. Temperatures became more uniform in August and decreased throughout September and October.

5.2.2 Cloud Cover and Solar Intensity

Sunlight is necessary for algae to undertake photosynthesis. In order to determine the time periods of increased photosynthetic activity, the cloud cover over Reno, NV, during the study period was examined and is presented in Figure 5-14. The red line details the daily percent cloud cover over the Reno-Tahoe International Airport weather station and the black line is the seven-day moving average of the percent cloud cover over the study period (4/12/11 to 10/18/11). During extended times of reduced cloud cover, photosynthetic activity was anticipated to increase. Cloud cover was typically greater than 50% from April 12th to June 7th.

The average cloud cover steadily decreased over the period from June 7th to June 21st to an average less than 25%. The cloud cover remained less than 25% until the beginning of September, when if ranged between 25% and 50% until the beginning of October. A decrease of cloud cover to below 25% is noticeable around September 27th. It was hypothesized that increased levels of photosynthetic activity would have been anticipated from June to September due to the combination of warmer surface temperatures and lower cloud cover. This hypothesis will be considered in the following sections.

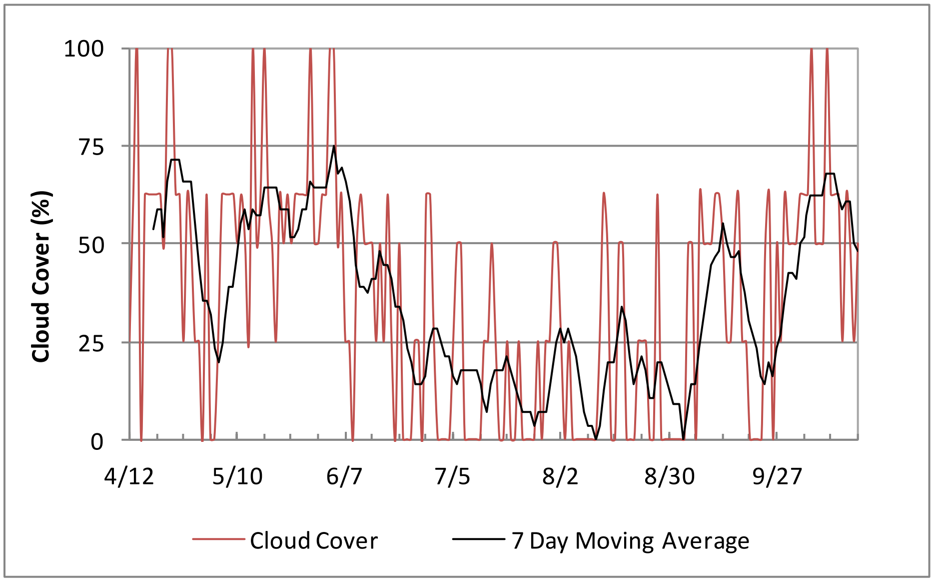

Figure 5-14: Percent Cloud Cover over Reno, NV throughout the Water Quality Study

5.2.3 Dissolved Oxygen and pH

When algae actively grow, they increase both dissolved oxygen and pH. These increases in pH and DO occur due to the consumption of inorganic carbon during photosynthesis and the release of oxygen into water, respectively (Chen and Durbin, 1994). Figures 5-15 and 5-16 present the variation in dissolved oxygen and pH throughout the sampling period at the water surface of locations A and B.

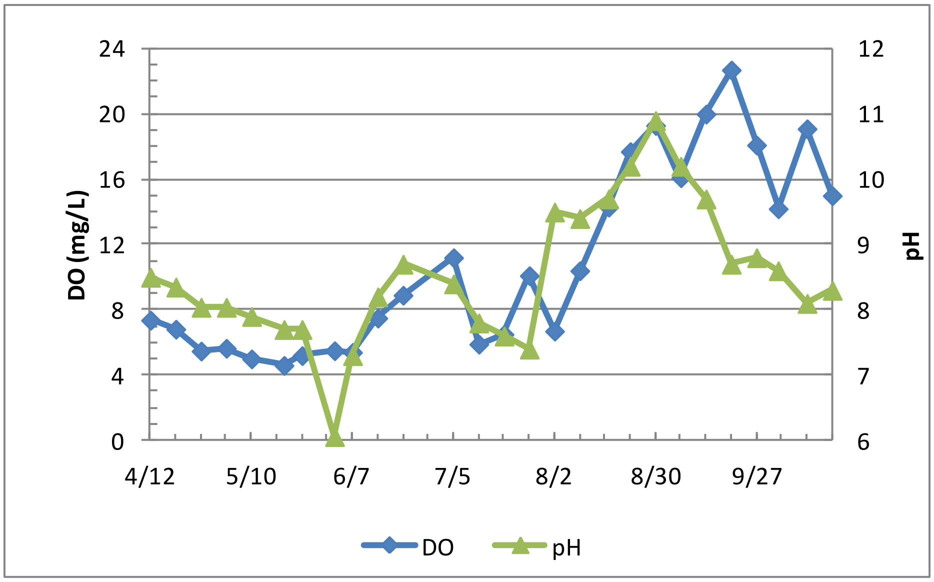

Figure 5-15: pH and Dissolved Oxygen Concentration at the Surface of Location A

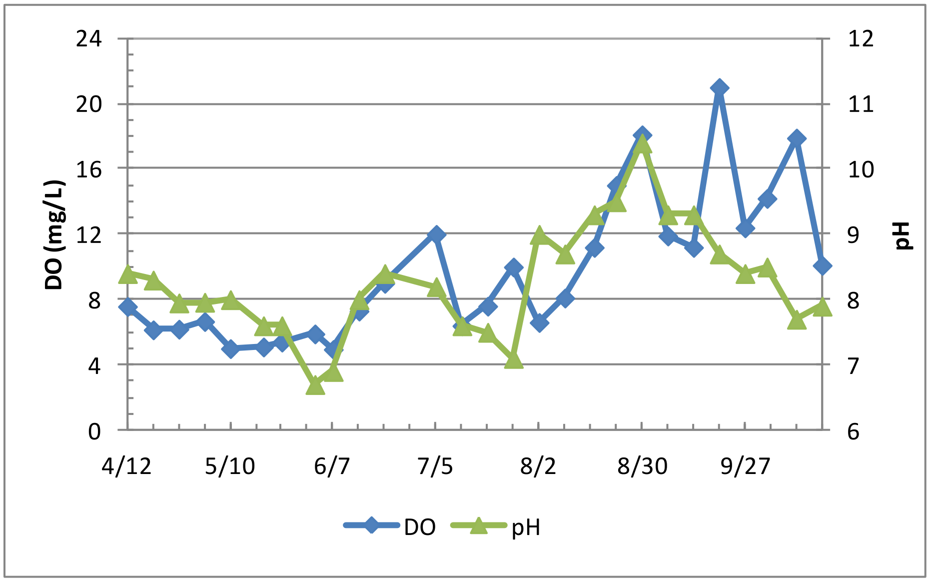

Figure 5-16: pH and Dissolved Oxygen Concentration at the Surface of Location B

For the period of April through August, the variation in pH and DO concentration are directly related. From April 12th to June 7th, DO concentrations decreased from approximately 8 mg O_2/L to 5 mg O_2/L and pH decreased from approximately 8 to 7. From June 7th to August 30th, DO concentrations increased from approximately 5 mg O_2/L to 18 mg O_2/L and pH increased from approximately 7 to 10.5. Throughout September and October, DO showed sporadic changes in concentration while pH steadily decreased. DO and pH levels observed in the reservoir throughout the study corresponded to levels observed by various researchers described in Section 2.2 (i.e., high DO and pH loads during periods of high algal growth).

The overall increase of DO and pH from June to September corresponds to the decreased cloud cover during this same time period suggesting increased rates of photosynthesis. The decrease in pH and DO in the beginning of September correspond to cloud cover greater than 50% and supports the case for a decrease in photosynthetic activity. As discussed in Section 2.2, algal growth may be inhibited at pH levels greater than 9 (Chen and Durbin, 1994). The monitored data levels in the reservoir show pH levels in excess of 9 from August 17th to September 13th and it is possible that, due to the high pH levels, algal growth and activity was inhibited during this time.

Table 5-6 summarizes the surface conditions in the reservoir that may have impacted photosynthetic activity. Based on the data, photosynthesis was thought to be suppressed from April 12th to June 7th, July 5th to July 26th, and August 30th to October 18th due to the increased cloud cover (supported by decreasing pH and DO concentrations). Photosynthesis was thought to have been most active from June 7th to July 5th and July 26th to August 30th due to decreased cloud cover (supported by increasing pH and DO concentrations). Location B had slightly larger changes in pH and DO compared to Location A, which is thought to be a result of the proximity of Location B to the inlet structure where STMWRF influent is pumped into the reservoir.

Table 5-6: Summary of Cloud Cover and Reservoir Surface Conditions during Possible Changes in Photosynthetic Activity

Time Period	Change in Cloud Cover (%)	Location A		Location B	
		Change in Dissolved Oxygen (mg/L)	Change in pH	Change in Dissolved Oxygen (mg/L)	Change in pH
April 12 – June 7	12.5	-2.0	-1.2	-2.6	-1.5
June 7 – July 5	-50.0	5.8	1.1	7.1	1.3
July 5 – July 26	12.5	-1.1	-1.0	-2.0	-1.1
July 26 – Aug 30	-16.0	9.2	3.5	8.1	3.3
Aug 30 – Oct 18	35.0	-4.3	-2.6	-8.0	-2.5

5.2.4 Free and Combined Chlorine

As described in Section 5.1.3, free chlorine (HOCl) and chloramines are present in plant effluent due to the addition of hypochlorous acid prior to the chlorine contact basin. It was hypothesized that all of the ammonia in oxidation ditch effluent was converted into chloramines due to the free chlorine residual concentrations measured. This suggests that all of the ammonia-nitrogen entering the reservoir is present as chloramines. Chloramines are notoriously unstable and undergo multiple abiotic degradation reactions. The most notable is the hydrolysis of monochloramine into HOCl and ammonia. Although the first-order rate of hydrolysis (7.6×10^{-2} h^{-1}) is slow compared to the kinetic rate of formation of monochloramine, at ammonia concentrations less than 2 mg N/L, the hydrolysis reaction dominates the monochloramine formation reaction (Harrington et al., 2003).

To understand the effect of chlorination on reservoir water quality, free chlorine and chloramine concentrations were measured at Locations A and B on March 14th through March 16th, 2012. The results of this analysis are presented in Table 5-7. Location A had no detectable concentrations of either free chlorine or chloramines, while Location B (near the effluent discharge pipe) had one instance of low free chlorine concentration (0.1 mg Cl_2/L). This suggests that all of the chloramines introduced into the reservoir degraded into ammonia and HOCl.

Table 5-7: Chlorine Concentrations in Huffaker Hills Reservoir

Site	Sample Collection Date	Free Chlorine (mg Cl_2/L)	Chloramines (mg Cl_2/L)
Location A	3/14/2012	0^*	0^*
	3/15/2012	0^*	0^*
	3/16/2012	0^*	0^*
Location B	3/14/2012	0.1	0^*
	3/15/2012	0^*	0^*
	3/16/2012	0^*	0^*

*Non-Detect Levels

5.2.5 Water Depth and Clarity

During the distribution season, the volume of water imported into the reservoir is approximately 2.5 million gallons per day (mgd), while the volume of water exported out of the reservoir is approximately 4.5 mgd. Due to the net water volume loss of 2 mgd, the surface water elevation in the reservoir is reduced throughout the distribution season. The magnitude of water elevation changes is presented in Figure 5-17.

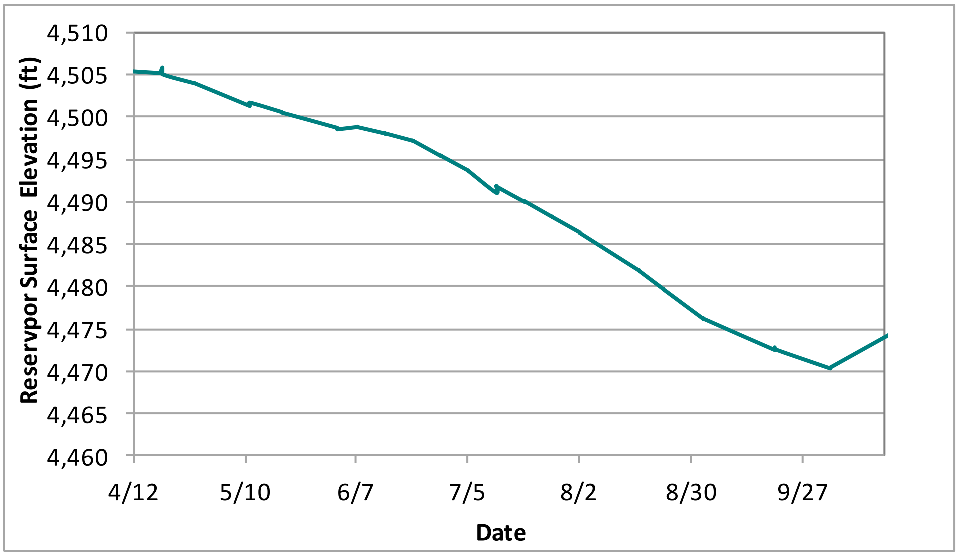

Figure: 5-17: Reservoir Water Depths of Locations A, B, and C

At the beginning of the study on April 12th, the surface water elevation of Huffaker Hills Reservoir was approximately 4,505 ft. Throughout the distribution season the surface water elevation steadily declined by 35 ft, reaching a minimum elevation of approximately 4,470 ft on October 4th. From October 4th until the sampling period, the surface water elevation increased by approximately 5 feet to an elevation of 4,475 ft due to a reduction in distribution water demand. Locations A, B, and C had initial water depths that were approximately 43 ft, 47 ft, and 22 ft, respectively. Due to the changing water surface elevation and the decreasing water depth, sample collection at Location C was not possible after August 2nd.

Reservoir water clarity was measured throughout the duration of the study and the data from Location A and B are presented in Figure 5-18. The clarity at both Location A and B are similar throughout the study with deviations between the two locations typically less than one foot. Water clarity decreased from approximately 15 feet at the beginning of the study to approximately 6 feet by May 30th. From June 7th to July 5th, water clarity increased to approximately 8 feet. By the end of the distribution season, reservoir water clarity decreased to approximately one foot. During this time, the reservoir surface water elevation was decreasing as depicted in Figure 5-17. It is possible that as the volume of water in the reservoir decreased, suspended solids in the upper levels of the reservoir were concentrated. The concentration of suspended solids coupled with increased algae growth near the reservoir surface resulted in a reduction of clarity.

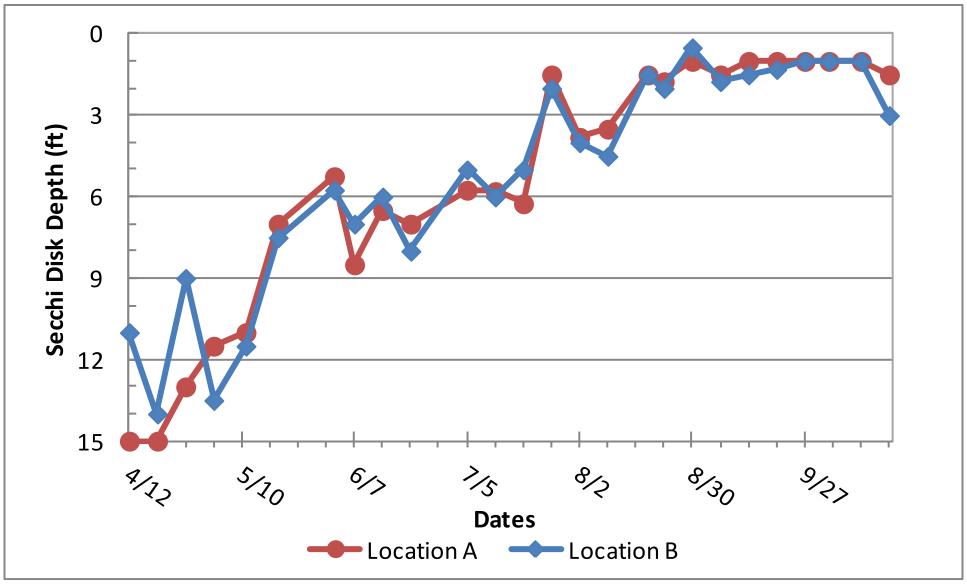

Figure: 5-18: Reservoir Water Clarity at Location A and B

5.2.6 Ammonia

The reservoir contains treated plant effluent which results in elevated concentrations of ammonia. Ammonia is beneficial to algal growth when it is present at concentrations less than 2.8 mg N/L (Abeliovich and Azov, 1976). Ammonia concentration profiles of the reservoir at Locations A and B are presented in Figure 5-19 and 5-20, respectively. The data depict increased concentrations of ammonia from April 12th to June 7th with increases from approximately 0.5 mg N/L to 2.0 mg N/L. Concentrations of ammonia decreased from June 7th to August 23rd from 2.0 mg N/L to 0 mg N/L, where ammonia reductions ranged from 21% to 100%. These data are consistent with results discussed in Section 2.2 where researchers observed ammonia reductions of 44% to 100% during periods of active algal growth.

Surface ammonia concentrations were typically lower than thermocline and bottom concentrations due increased microbial activity and potential volatilization. The ammonium/ammonia (NH_4^+/NH_3) species have a pK_a value of 9.25. At pH values near or exceeding the pK_a, the high Henry's coefficient of ammonia (k_H = 0.017 atm/M) would allow for ammonia to be removed by volatilization. In order to determine the differences in concentrations at the various depths in the reservoir, concentrations at the bottom and thermocline were divided by the concentrations measured at the surface to normalize the data. The results are presented in Figures 5-21 and 5-22 for Locations A and B, respectively. Values less than 1.0 indicate concentrations less than the surface and values greater than 1.0 indicate concentrations greater than at the water surface. From April 12th to June 7th, ammonia concentrations were typically uniform throughout the reservoir profile. From June 7th to August 30th, concentrations at the bottom were approximately three times higher than the surface concentration. From September to October, ammonia concentrations throughout the reservoir profile at Location B were typically uniform.

In Figures 5-19 through 5-21, gaps in data from August 30th forward are due to the changing water depth in the reservoir as discussed in Section 5.2.5. Surface samples were collected throughout the duration of the study; however, thermocline and bottom samples were not always available as the reservoir depth decreased.

As discussed previously, volatilization may have aided in the removal of ammonia from the reservoir at pH levels at or exceeding the pK_a of the ammonium/ammonia couple. From Figures 5-15 and 5-16, reservoir pH was at or above 9.25 from August 2nd to September 13th. It is possible that along with increased microbial uptake of ammonia, volatilization aided in the low, near zero concentrations of ammonia present during this time.

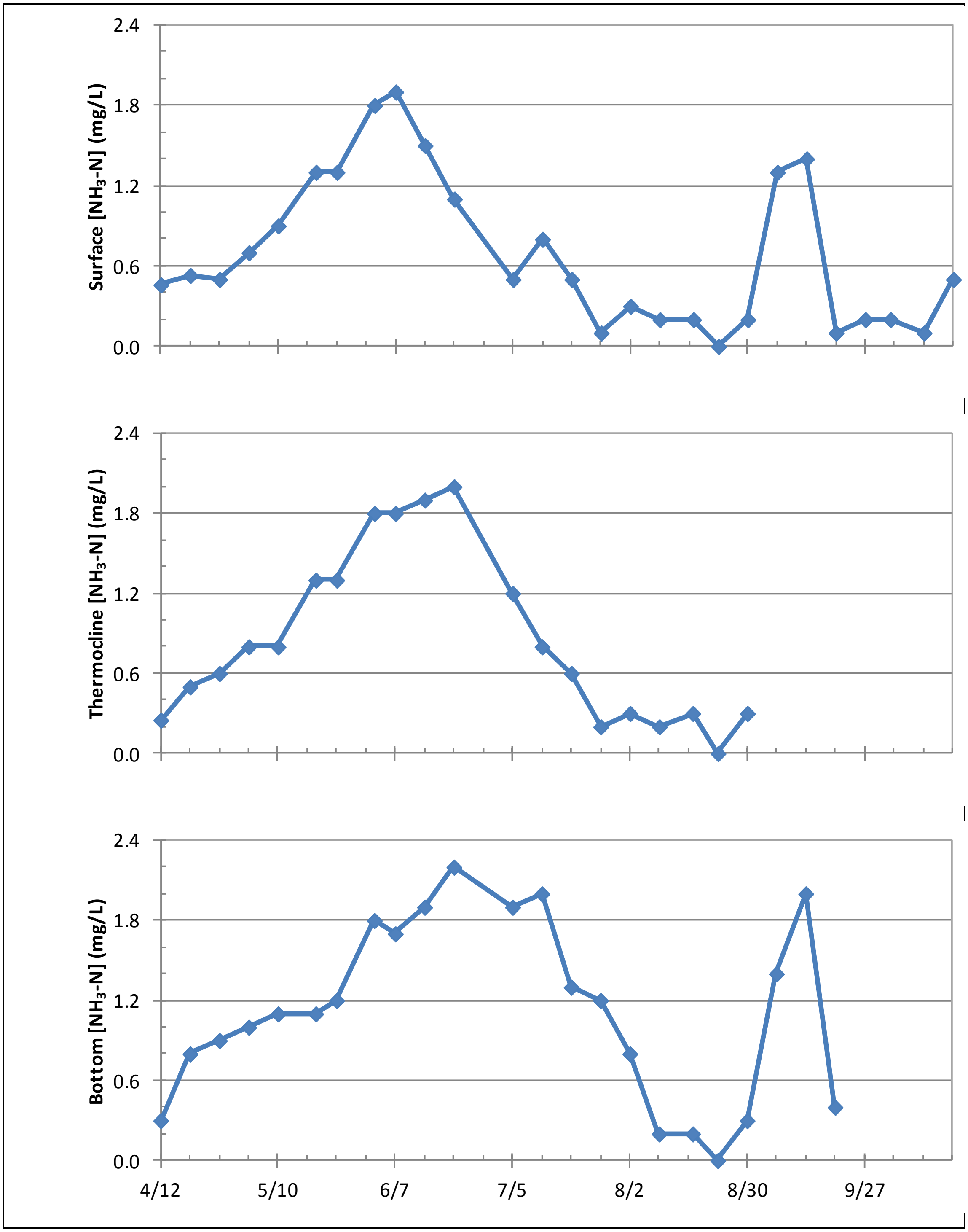

Figure 5-19: Ammonia Concentration Profile at Location A throughout Water Quality Study

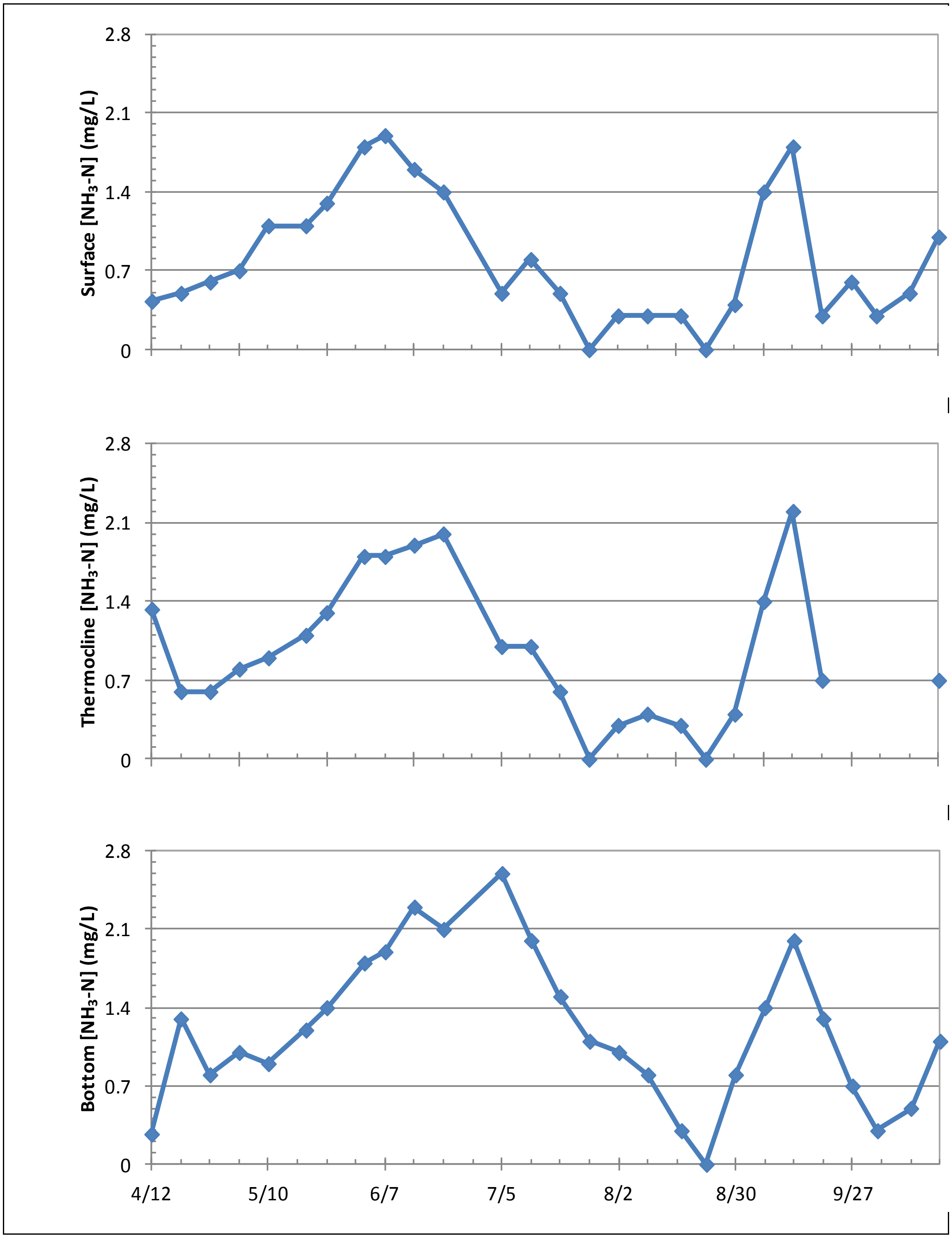

Figure 5-20: Ammonia Concentration Profile at Location B throughout Water Quality Study

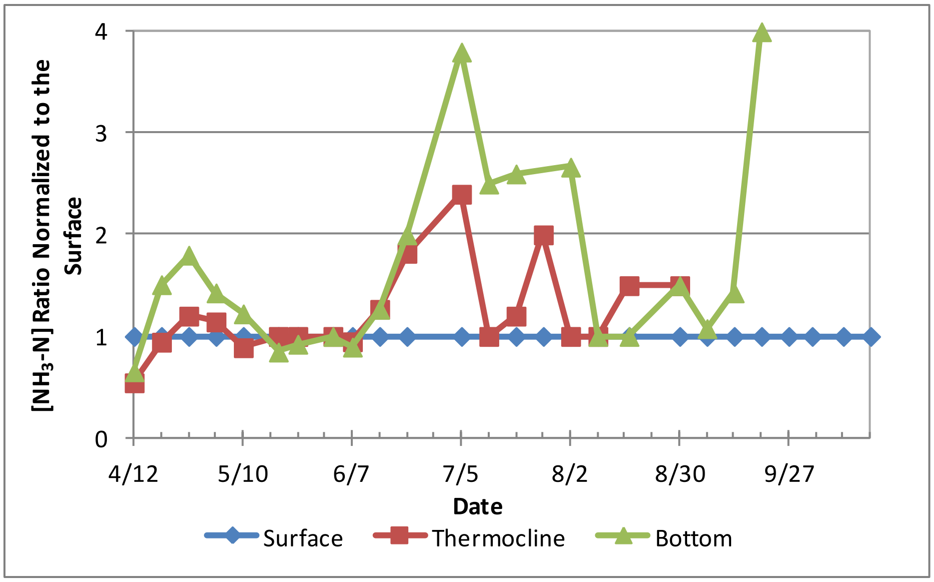

Figure 5-21: Normalized Ammonia Concentrations to Location A Surface

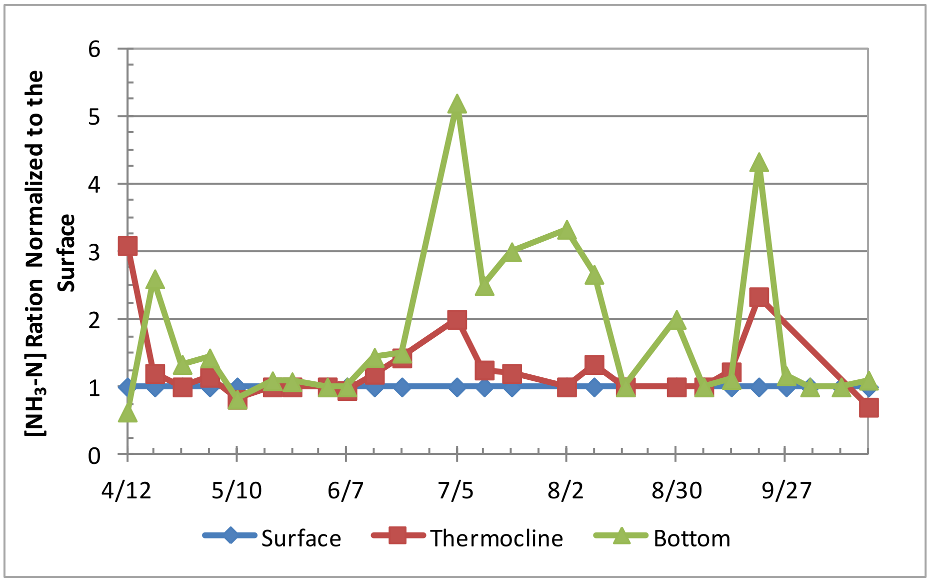

Figure 5-22: Normalized Ammonia Concentrations to Location B Surface

5.2.7 Phosphate

Phosphorus is a necessary growth nutrient for microorganisms, and is typically the limiting nutrient in most natural environments (Jansson, 1988). As discussed in Section 2.2, the nitrogen to phosphorus ratio (N:P) is often used to determine whether an aquatic system is either nitrogen- or phosphorus-limited. Due to the complexities between varying strains of algae, a representative N:P value has not been determined for algae. Instead, studies have determined an N:P range of 5-15 that is most frequently encountered in algae (Rhee and Gotha, 1980). Variations in the N:P ratio at Locations A and B are presented in Figure 5-23. The nitrogen portion of the N:P ratio is the addition of ammonia and nitrate concentrations, while the phosphorus portion of the N:P ratio is the concentration of orthophosphate. The maximum N:P ratio of 2.3 occured from April 12th to June 7th. This maximum value is less than the lower limit of the ideal N:P range of 5-15 for algae. From June 7th to August 23rd, the N:P steadily decreased to a minimum value near zero at Locations A and B. During September and October the N:P increased to 1.3. These comparatively low N:P values suggest that nitrogen was the limiting nutrient in the reservoir.

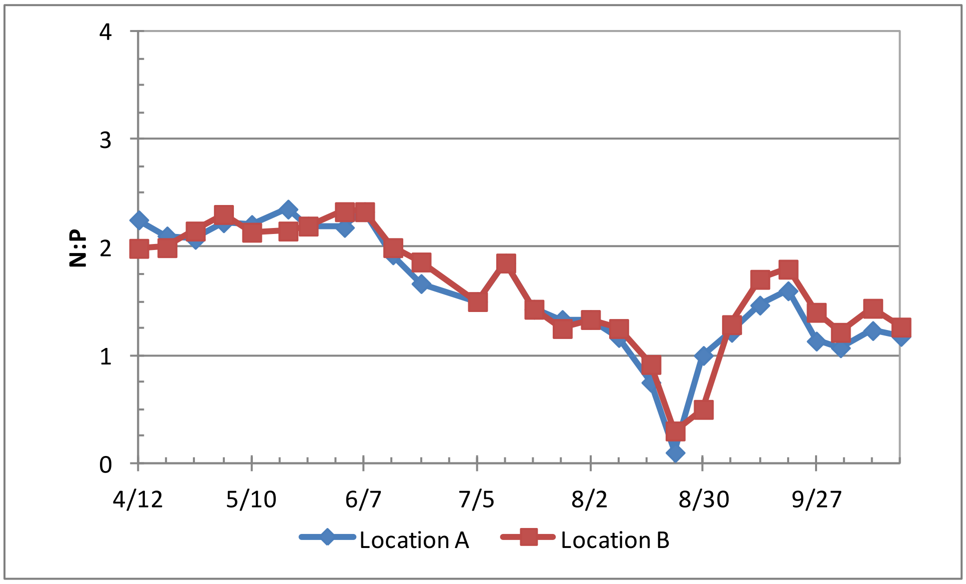

Figure 5-23: N:P at the Surface of Locations A and B

Orthophosphate concentrations had negligible variations throughout the reservoir profile over the course of the study. The average concentrations and standard deviations for orthophosphate are presented in Figures 5-24 and 5-25 at Locations A and B, respectively. Orthophosphate concentrations increased from 1.3 mg P/L to 1.5 mg P/L from April 12th to June

7th. Concentrations decreased to a low of 1.0 mg P/L by August 23rd, with observed orthophosphate reductions ranging from 0% to 33%. The orthophosphate reductions were less than reductions observed by research discussed in Section 2.2 where researchers observed decreases in orthophosphate ranging from 11% to 88%. However, the system they were sampling had a higher N:P ratio and higher influent concentrations of nutrients. During September and October, orthophosphate concentrations reached a maximum of 1.7 mg P/L.

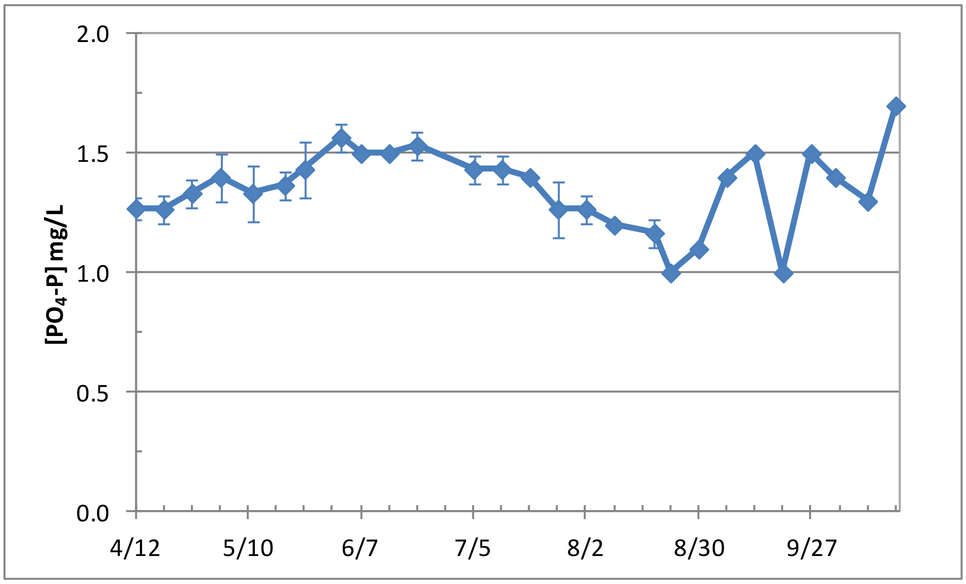

Figure 5-24: Average Orthophosphate Concentration at Location A

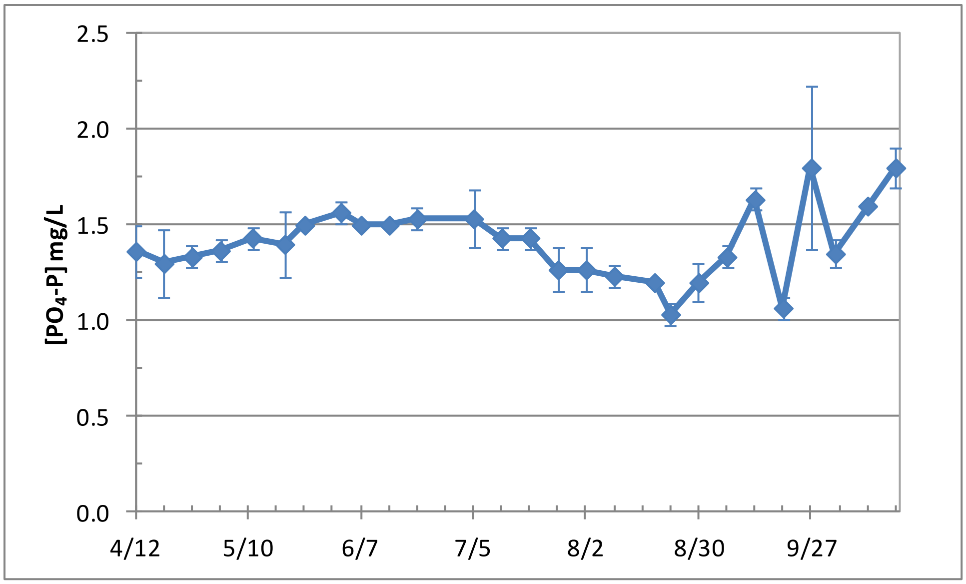

Figure 5-25: Average Orthophosphate Concentration at Location B

5.2.8 Reservoir Summary

Conditions in the reservoir from April 12th to June 7th indicated that algae were not photosynthetically active. Cloud cover was greater than 50% on average while both pH and DO concentrations were observed to decrease. Due to the low photosynthetic activity during this time period, both ammonia and phosphate concentrations increased. Starting in early June, cloud cover began to decrease to an average of less than 25% and both pH and DO concentrations increased. From June 7th to August 23rd, both ammonia and orthophosphate concentrations decreased markedly suggesting elevated levels of algal and photosynthetic activity. During this time, concentrations of ammonia fell below detection limits across the reservoir profile (including lower levels of the reservoir).

5.3 Effects of Chemical Coagulation on Algae Removal

5.3.1 Reservoir Water Quality Study

The reservoir surface turbidity throughout the duration of the study is presented in Figure 5-26. The red lines correspond to the time period when jar test samples were collected and the green lines correspond to the time period when filtration samples were collected.

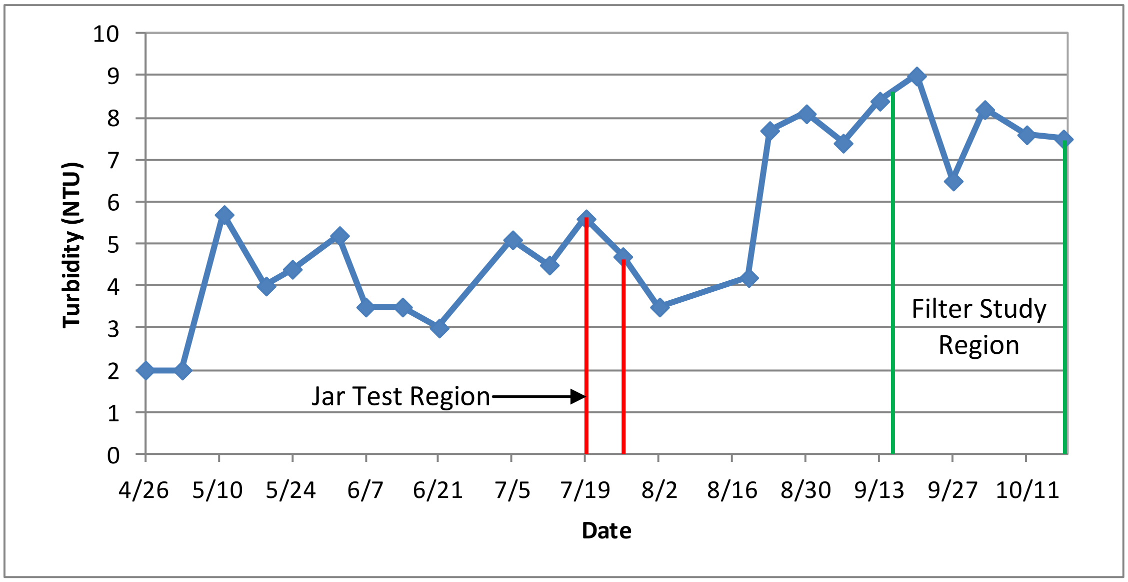

Figure 5-26: Variations in Surface Turbidity in Huffaker Hills Reservoir at Location B

5.3.2 Jar Test Experiments

Jar testing was conducted at the end of July to determine the optimum coagulant dose for a mixture of reservoir water and secondary effluent. Table 5-8 summarizes the initial conditions of sample water collected for jar testing.

From Figure 5-26 and Table 5-8, the initial turbidity of the water used during jar testing closely compares with the surface turbidity of the water at the surface of the Huffaker Hills Reservoir.

Table 5-8: Initial Conditions of Jar Test Samples

Date Sample Collected	pH	Initial Turbidity (NTU)
July 20, 2011	7.3	5.2
July 22, 2011	7.0	4.1
July 26, 2011	7.2	4.3
July 21, 2011	7.3	3.8

Figure 5-27 presents the 95% confidence interval of the observed reduction in settled water turbidity during jar testing calculated about the mean for various alum doses after a settling period of 12 minutes. At the lowest dose of alum at 6.3 mg/L, the turbidity removed through settling was less than the control which did not have any alum added. This most likely occurred due to the formation of pin-point floc particles which were too small to settle out of the water during the 12 minute settling period. Other studies demonstrated that high doses of alum in excess of 100 mg/L are often necessary for high algal removal efficiencies (Friedman, 1977). The doses used during this jar test study reached a maximum of 44 mg/L which has the potential to remove as much as 45% of the turbidity on average with coagulation and settling as the sole removal mechanisms. Table 5-9 summarizes the 95% confidence interval for alum.

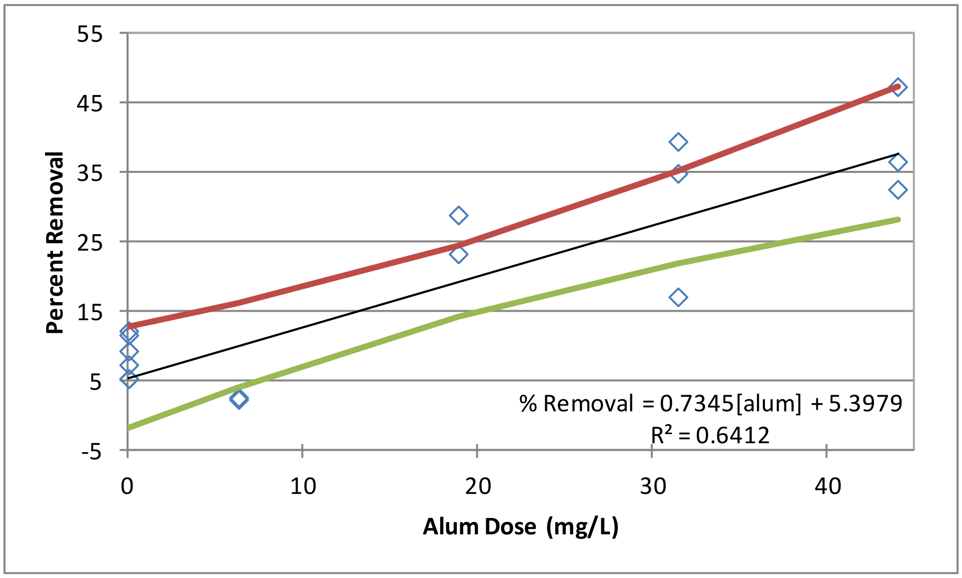

Figure 5-27: 95% Confidence Interval of Percent Turbidity Removal during Alum Jar Testing

Table 5-9: % Confidence Interval for Percent Turbidity Removal During Jar Testing With Alum

Dose (mg/L)	Lower Limit (%)	Calculated Mean (%)	Upper Limit (%)
0	-1.9	5.4	12.7
6.3	3.9	8.3	16.1
18.9	14.2	14.1	24.4
31.5	21.9	20.0	35.1
44	28.2	25.7	47.3

The 95% confidence interval of the observed reduction in settled water turbidity during jar tests using ferric chloride after a settling period of 12 minutes is presented in Figure 5-28. At the 18 mg/L dose, one data point exhibited a removal efficiency less than the control dose. A possible reason for this is that particle sizes were formed which were too small to settle out of suspension within the 12 minute settling period. Table 5-10 summarizes the 95% confidence interval for $FeCl_3$ jar tests.

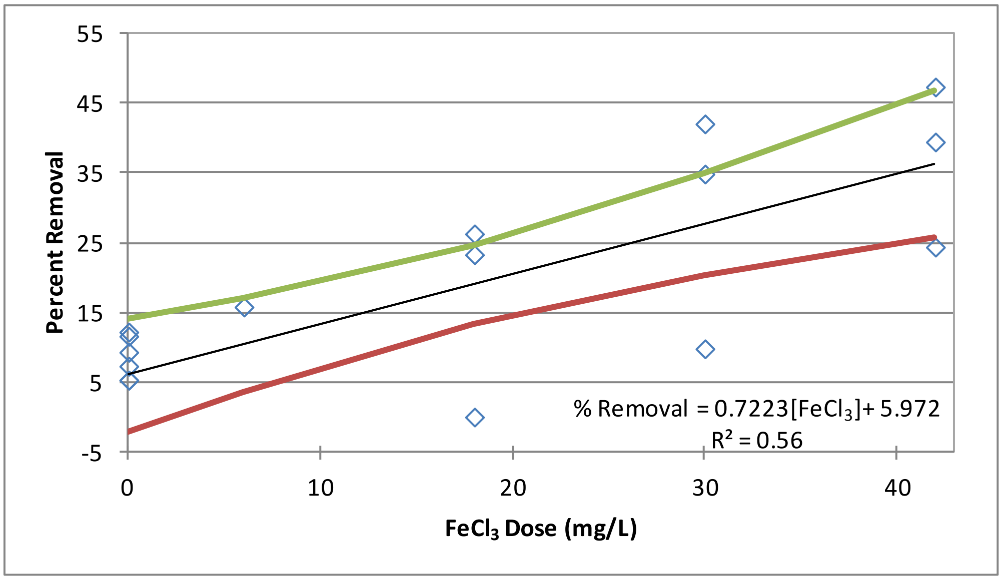

Figure 5-28: 95% Confidence Interval for Percent Turbidity Removal during Jar Testing With $FeCl_3$

Table 5-10: 95% Confidence Interval for Percent Turbidity Removal During Jar Testing With $FeCl_3$

Dose (mg/L)	Lower Limit (%)	Calculated Mean (%)	Upper Limit (%)
0	-2.2	6.0	14.1
6	3.5	8.6	17.1
18	13.3	13.8	24.6
30	20.3	19.0	35.0
42	25.7	24.2	46.9

The addition of alum and $FeCl_3$ typically reduces the pH due to the formation of the hydrolysis species which consume hydroxide ions. Table 5-11 presents the average pH change of the water as a result of coagulant addition during jar testing. As anticipated, the magnitude of the pH change typically increased as the dose of coagulant increased since more hydroxyl ions were removed from solution.

Table 5-11: pH Changes after Jar Testing with Alum and $FeCl_3$ Jar Tests

Alum		$FeCl_3$	
Dose (mg/L)	pH Change	Dose (mg/L)	pH Change
6.3	-0.2	6	0.1
18.9	-0.25	18	-0.2
31.5	-0.4	30	-0.45
44	-0.55	42	-0.55

5.3.3 Filtration Study

Coagulant doses of approximately 0, 9, 18, and 27 mg/L of alum and $FeCl_3$ were used during the pilot-scale filter study over the period from September 16, 2011, through November 1, 2011. Each targeted dose was replicated three times and it is believed that these doses represent the range that the Washoe County Department of Water Resources would be most likely to use during full-scale coagulation/filtration operations.

The effect of coagulant addition on pH was measured during certain filter runs and the results are summarized in Table 5-12. Typically, pH changes increase as the coagulant dose is increased as more hydroxyl ions are removed from solution. Tables 5-13 and 5-14 contain the raw data for the alum and $FeCl_3$ filter runs, respectively, and show the initial and final pH of coagulated filter water.

Table 5-12: Variation of pH of Filter Influent after Coagulant Addition

Alum		**$FeCl_3$**	
Dose (mg/L)	**pH Change**	**Dose (mg/L)**	**pH Change**
9.4	-0.1	9	-0.1
18.9	-	18	-0.1
28.3	-0.55	27	-0.55

Linear regressions were performed for the coagulation and filtration data. Figures 5-29 and 5-30 are box plots which show the distribution of the raw data of alum and $FeCl_3$, respectively. The boxes shown describe the interquartile range which represents the degree of dispersion of the data. The larger the spread of the box, the larger the dispersion of data. The line dividing each box is the median of the data. The lines coming off the box, also called whiskers, show the minimum and maximum data points. For each dose greater than the control, the edge of each whisker and the median are equivalent to the three data points. Figures 5-31 and 5-32 contain the 95% confidence and 95% prediction intervals of alum and $FeCl_3$, respectively.

Table 5-13: Alum Filter Data

				0 mg/L		15 mg/L	
Date	**Tank Turbidity (NTU)**	**Initial pH**	**Final pH**	**Turbidity Percent Removal**	**Loading Rate (gpm/ft^2)**	**Turbidity Percent Removal**	**Loading Rate (gpm/ft^2)**
9/28/2011	18.8	8.3	8.3	11.8	4.7	22.8	5.5
10/12/2011	5.7	7.7	7.5	30.1	5.1	39.1	4.9
10/24/2011	7.6	-	-	42.3	5.1	73	4.9
				0 mg/L		**30 mg/L**	
Date	**Tank Turbidity (NTU)**	**Initial pH**	**Final pH**	**Turbidity Percent Removal**	**Loading Rate (gpm/ft^2)**	**Turbidity Percent Removal**	**Loading Rate (gpm/ft^2)**
9/16/2011	12.6	-	-	10.7	5.7	39.4	4.7
10/13/2011	6.5	-	-	37.6	5	59.7	4.9
10/21/2011	20.3	-	-	70.4	4.8	79.8	4.5
				0 mg/L		**45 mg/L**	
Date	**Tank Turbidity (NTU)**	**Initial pH**	**Final pH**	**Turbidity Percent Removal**	**Loading Rate (gpm/ft^2)**	**Turbidity Percent Removal**	**Loading Rate (gpm/ft^2)**
9/26/2011	13.4	-	-	22.7	5.1	64.2	4.8
10/11/2011	7.7	8.4	7.7	35.3	5.1	58.4	5.1
10/25/2011	9.0	8.7	8.3	53.2	5.1	87	3.9

Table 5-14: $FeCl_3$ Filter Data

				0 mg/L		15 mg/L	
Date	**Tank Turbidity (NTU)**	**Initial pH**	**Final pH**	**Turbidity Percent Removal**	**Loading Rate (gpm/ft^2)**	**Turbidity Percent Removal**	**Loading Rate (gpm/ft^2)**
9/19/2011	18.2	8.2	8.1	11.2	4.6	21.4	5.9
10/14/2011	15.2	8.3	8.2	44	5.2	71.8	5.8
11/1/2011	4.0	-	-	36.7	5.1	63.9	4.6
				0 mg/L		**30 mg/L**	
Date	**Tank Turbidity (NTU)**	**Initial pH**	**Final pH**	**Turbidity Percent Removal**	**Loading Rate (gpm/ft^2)**	**Turbidity Percent Removal**	**Loading Rate (gpm/ft^2)**
9/29/2011	10.4	8.4	8.3	29.8	4.9	73.4	4.6
10/17/2011	8.1	-	-	39	5.1	60.5	5
10/31/2011	7.0	-	-	56.6	5.1	80.1	4.7
				0 mg/L		**45 mg/L**	
Date	**Tank Turbidity (NTU)**	**Initial pH**	**Final pH**	**Turbidity Percent Removal**	**Loading Rate (gpm/ft^2)**	**Turbidity Percent Removal**	**Loading Rate (gpm/ft^2)**
9/23/2011	14.4	8.7	8.3	25.6	5	68.4	4.3
10/4/2011	10.3	8.4	7.7	31	5	68.2	4.8
10/20/2011	10.2	-	-	55.6	5	80	4.1

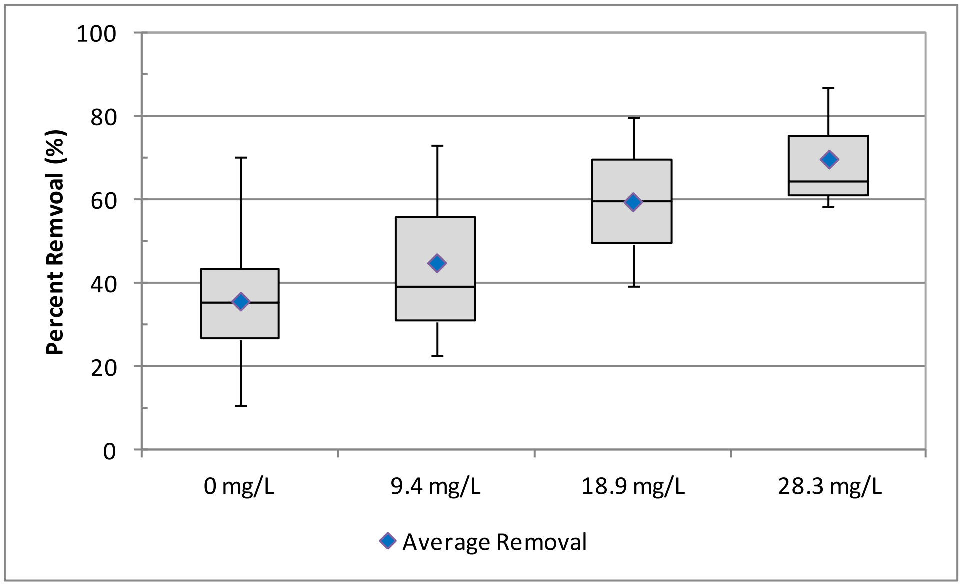

Figure 5-29: Variation of Turbidity Removal with Alum Dose during Filtration

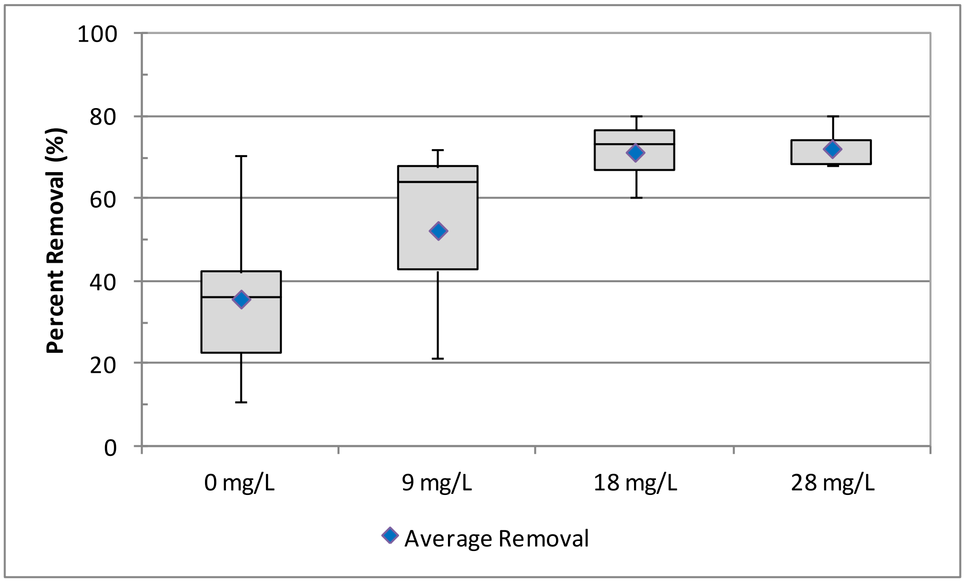

Figure 5-30: Variation of Turbidity Removal with $FeCl_3$ Dose during Filtration

As can be seen in Figures 5-29 and 5-30, the variability of the data decreased as the dose of both coagulants increased. This suggests that turbidity removal will consistently increase as the doses of coagulant increases, according to the observed data. It is noteworthy that the removal efficiencies observed during filtration were markedly higher for both alum and $FeCl_3$

compared to jar testing alone. This is due to settling being the driving force of removal during jar tests while particle capture and immobilization was the driving force of removal during filtration.

In Figures 5-31 and 5-32, the 95% confidence interval and the 95% prediction intervals of alum and $FeCl_3$ coagulation are presented, respectively. The confidence interval represents, with 95% confidence, the interval that would contain the average of future turbidity removal for a specific coagulant dose. On the other hand, the prediction interval represents, with 95% confidence, the interval at which a single turbidity removal event would occur at a particular coagulant dose. The narrow confidence intervals in Figure 5-31 and 5-32 demonstrate that the average turbidity removal for alum and $FeCl_3$ would be easily predicted. However, the broad range of the prediction intervals demonstrate that a single event could have a wide range of potential removal efficiencies.

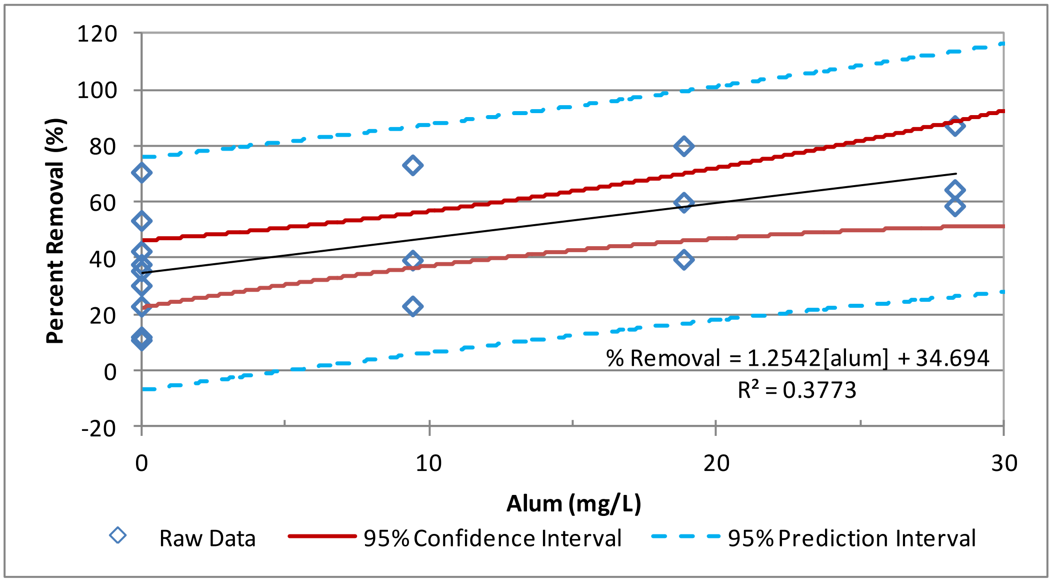

Figure 5-31: Confidence and Prediction Intervals of Alum Filtration Data

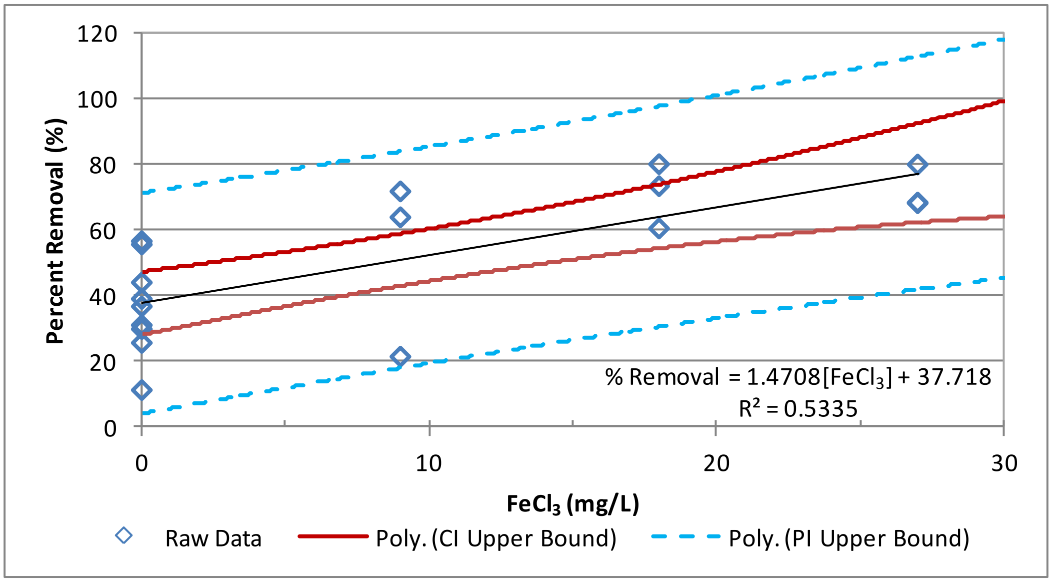

Figure 5-32: Confidence and Prediction Intervals of FeCl$_3$ Filtration Data

From Figures 5-31 and 5-32, FeCl$_3$ has both narrower confidence and prediction intervals, and the potential removal capabilities are greater when compared to alum. For example, at an alum dose of 20 mg/L, the confidence interval is approximately 45% to 70%, and the prediction interval is approximately 22% to 97%. The confidence interval and prediction intervals for a FeCl$_3$ dose of 20 mg/L are approximately 55% to 80% and 30% to 100%, respectively. This suggests that FeCl$_3$ is expected to have greater average and individual removal efficiencies compared to alum.

As depicted in Figures 5-29 and 5-30, the control column had highly variable removal, ranging from approximately 10 to 70% throughout the filtration study as indicated by the spread of the whiskers. This is likely a result of the variations in the influent water quality where turbidity values ranged from 4.1 to 20.3 NTU. Figure 5-33 presents the percent removal in the control column throughout the filter column study plotted on the left-Y axis and the influent turbidity throughout the study plotted on the right Y-axis.

The turbidity removal within the control filter column (no coagulant) increased steadily throughout the study while influent turbidity fluctuated between 5 and 20 NTU throughout the study. A linear trendline was determined for the control column removal data and the resulting R^2 value (0.68) indicates a reasonable fit to the data. It is apparent that the filtration columns worked more efficiently as the testing progressed. Since the study was conducted in the field several factors were unable to be controlled. For example, temperature fluctuations occurred over the 46 day study which may have influenced algae growth and decay.

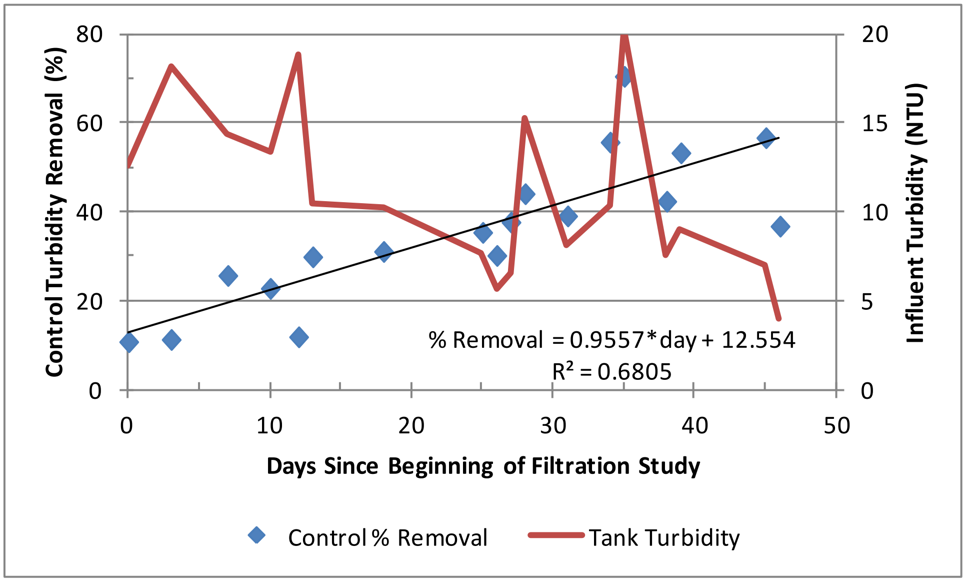

Figure 5-33: Variation of Filter Influent Turbidity at Location B and Turbidity Removal in Control Filter Column

Fluctuations in pH throughout the study may have inhibited the optimal formation of aluminum and iron precipitates. The operating range for aluminum hydroxide precipitation is in a pH range of 5.5 to 7.7 with minimal solubility occurring at a pH of approximately 6.2. The operating range for iron precipitation is in a pH range of 5 to 8.5 with minimal solubility occurring at a pH of approximately 8.0 (Crittenden, 2005). As seen in Tables 5-13 and 5-14, the final pH of both alum and $FeCl_3$ filter runs are at the upper reaches of the operating range and typically greater than the pH of minimal solubility.

Figure 5-34 shows that the effluent from the filter column receiving coagulant had consistently lower turbidity values than the control filter column. The increase in removal over the control for each coagulant run throughout the study is plotted on the left Y-axis and the daily minimum air temperature and reservoir surface temperatures are plotted on the right Y axis.

Both the influent turbidity and the change in percent removal over the control decreased regardless of coagulant dose until approximately day 25 of the filter study. At this point the change in percent removal over the control steadied regardless of the coagulant dose. The temperature data in Figure 5-34 shows a sharp decrease in both minimum air temperature around day 15 and a constant decrease in reservoir surface water temperature starting at the beginning of the study. The near freezing air temperatures may have had an impact on algae growth and/or decay and could have contributed to the very gradual decline in turbidity observed in the reservoir in Figure 5-28, the increase in percent turbidity removal for the control filter column observed in Figure 5-33, and the change in percent turbidity removal over the control observed in Figure 5-34.

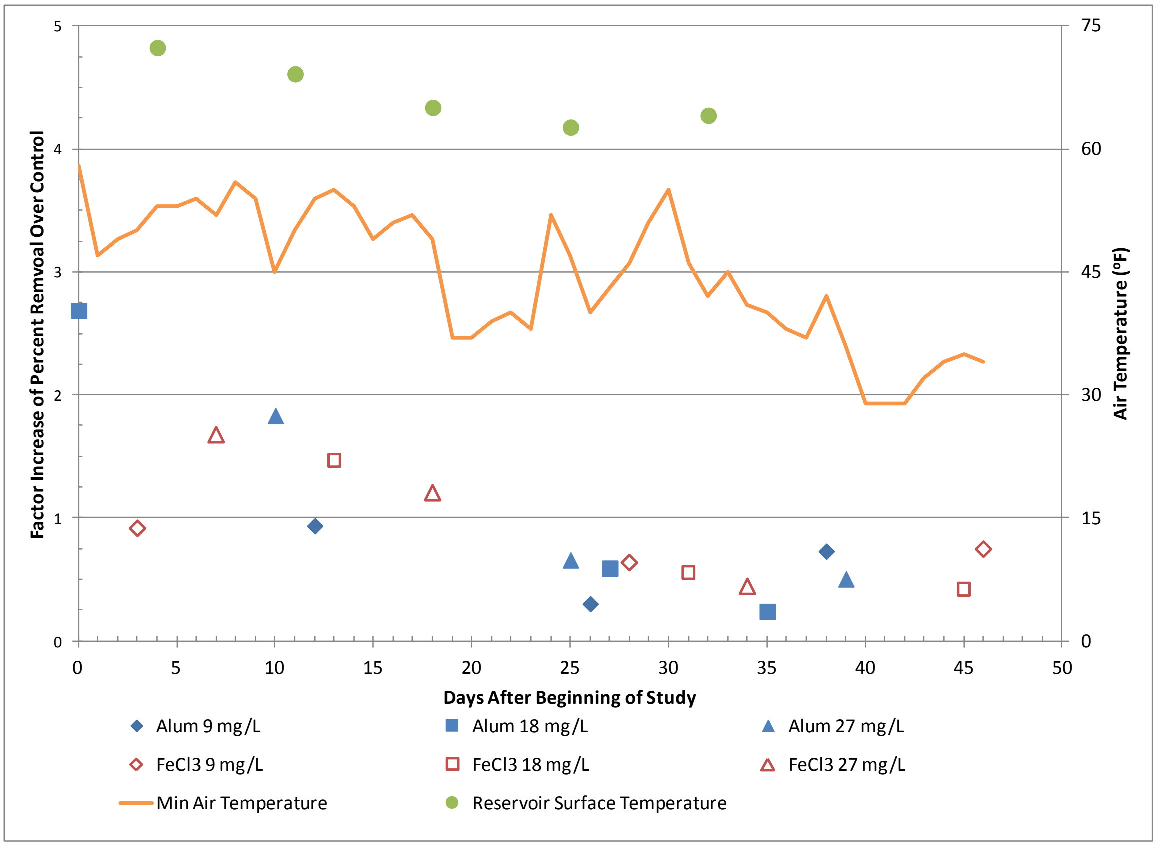

Figure 5-34: Percent Removal over Control of Alum and $FeCl_3$ with Temperature Fluctuations

Due to the dropping temperature and corresponding decrease in demand for reclaimed water, the volume of water exported daily to the distribution system decreased throughout the filtration study. These data are presented in Figure 5-35.

The number of pumps exporting water is dependent on the total amount of water exported. When the volume demand is lowered, the number of pumps needed to distribute water is decreased. This reduces the flow out of the reservoir and may have contributed to the change of the influent turbidity during the filtration study.

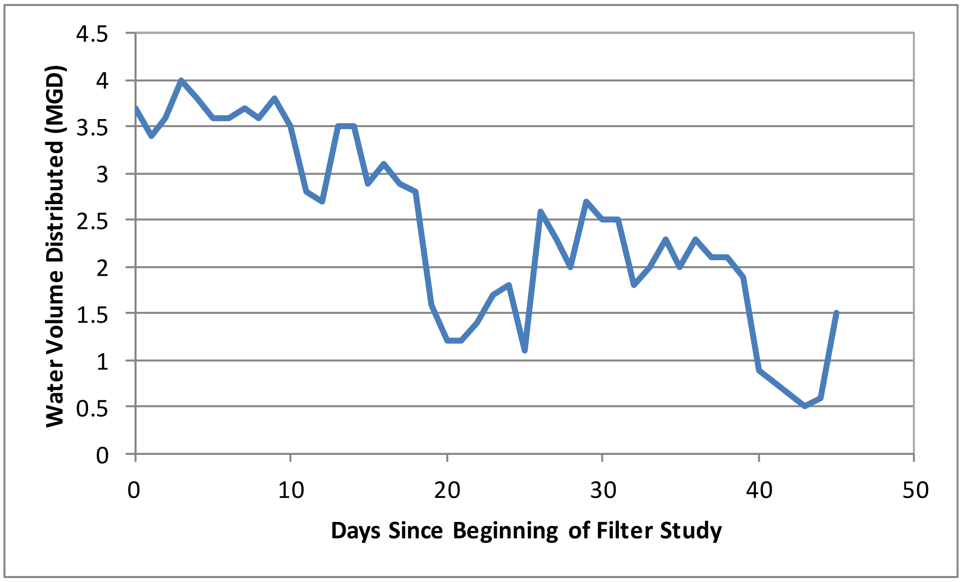

Figure 5-35: Volume of Water Exported From Huffaker Hills Reservoir during Filter Study

Another factor that may have contributed to the variations of turbidity removal with time was the characteristics of the filter sand which may have changed throughout the study. The results of a sieve analysis performed on sand removed from the control column and fresh unused sand are displayed in Table 5-15. From these values the coefficient of curvature (C_c) and the coefficient of uniformity (C_u) were calculated to determine the similarity of the sand in the control filter column and the clean sand. The sand from the control filter column did have slightly smaller particle diameters for d_{10}, d_{30}, and d_{60} which may partially account for the increase in the removal efficiencies of the control column over time. The distribution of particle sizes was consistent for both the control and clean sand as shown in Table 5-15 by C_c and C_u.

Table 5-15: Particle Distribution Results

	Clean Sand	**Control Sand**
d_{10} (mm)	1.35	1.2
d_{30} (mm)	1.6	1.45
d_{60} (mm)	1.9	1.7
C_c	0.7	0.7
C_u	1	1

It is worth noting that the results presented in this section were produced from down flow gravity filter columns that were backwashed at the end of each test run. This caused removal efficiencies to decrease during each individual test as the filter media would become clogged with the coagulated influent. The filters at STMWRF are continuously backwashed up-flow filters and clearly do not have the same filter hydraulics as the ones used in the pilot-scale study. Along with the difference in the filter configuration, Washoe County has determined that coagulation would most likely be implemented during the warmest months of the year from June 1st to October 1st.

Should coagulation be chosen as a suitable method of enhancing turbidity removal during filtration, a coagulant and dose is needed which provides consistent removal despite the variability of influent water quality. Throughout the pilot scale filtration study, the influent water turbidity fluctuated throughout testing as shown in Figure 5-33. Due to these changes, it is important to use a coagulant dose with minimal variability in turbidity removal. According to Figures 5-29 and 5-30 the distribution of removal efficiency narrows as the coagulant dose is increased. This suggests that higher doses of both coagulants will produce more reliable turbidity removal regardless of the influent water turbidity. Due to the pH dependence of metal precipitation during coagulation, however, pH adjustment may be necessary to achieve reliable removal with widely fluctuating influent water quality.

5.4 Reclaimed Water Distribution System

5.4.1 Nutrients

5.4.1.1 Ammonia

As described in Section 5.1.3, oxidation ditch and reservoir effluent was chlorinated prior to release into the distribution system, converting ammonia into chloramines. Free and combined chlorine concentrations in the distribution system were collected on several days throughout the study by Washoe County employees. Free chlorine and chloramine concentrations are presented in Table 5-16 and 5-17, respectively. Locations closest to the plant (Trademark) typically exhibited the highest concentrations while locations further from the plant (Field Creek, Arrow Creek) exhibited the lowest concentrations. This is most likely due to chemical and biological reactions which degrade disinfectants within the system.

Table 5-16: Free Chlorine Concentrations throughout Distribution System

	Free Chlorine (mg Cl_2/L)				
Date	**Trademark**	**Wilbur Mae**	**Rio Wrangler**	**Field Creek**	**Arrow Creek**
6/21/2011	3.9	3.0	2.9	2.0	0.1
6/28/2011	4.3	3.8	3.4	1.7	0.6
7/5/2011	1.3	1.2	0.8	0.9	0.8
7/19/2011	5.9	3.0	4.7	0.8	0.5
7/26/2011	3.5	2.1	3.7	0.8	0.7

Table 5-17: Chloramine Concentrations throughout Distribution System

	Chloramines (mg Cl_2/L)				
Date	**Trademark**	**Wilbur Mae**	**Rio Wrangler**	**Field Creek**	**Arrow Creek**
6/21/2011	2.9	1.2	1.1	0.2	0.5
6/28/2011	3.0	2.1	3.1	1.4	1.4
7/5/2011	0.6	1.7	2.3	0.3	0.8
7/19/2011	1.8	2.2	1.9	1.1	0.8
7/26/2011	2.1	1.7	1.4	0.5	0*

*non-detect levels

As presented in Section 3.5.1.1, ammonia measured in the laboratory is converted into monochloramine by the reaction with hypochlorous acid. Thus, chloramines present in sample water will be included in the ammonia concentrations reported by the instrument. Due to concentrations of free chlorine present in the distribution system throughout the study, it is hypothesized that ammonia concentrations measured in the lab are actually present as chloramines.

The average chloramine concentration throughout the distribution system and the surface concentration at Location B are presented in Figure 5-36. Chloramine concentrations increased from April 26th to June 2nd from 0.7 mg N/L to 1.9 mg N/L in the distribution system, corresponding to an increase in reservoir ammonia concentrations during the same time period from 0.5 mg N/L to 2.0 mg N/L. From June 7th to August 23rd, average chloramine concentrations decreased to 0.1 mg N/L in the distribution system while reservoir ammonia concentrations reached non-detect levels by this time. On September 6th, a high chloramine concentration of approximately 3.0 mg N/L in the distribution system corresponded to spike in reservoir concentration equal to 2 mg N/L.

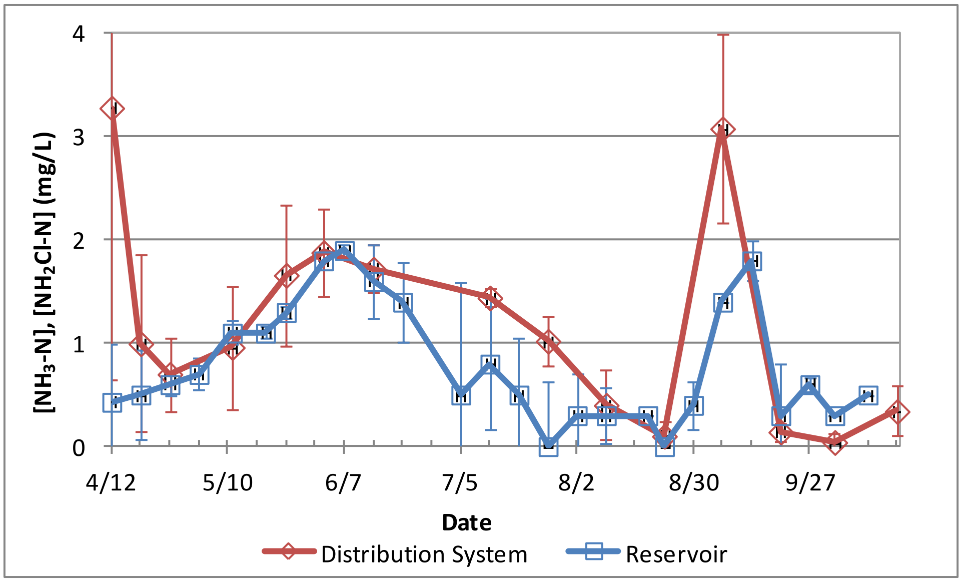

Figure 5-36: Chloramine Concentration in the Distribution System and Ammonia Surface Concentrations at Location B

5.4.1.2 Orthophosphate

The average orthophosphate concentrations throughout the distribution system and the surface concentration at Location B in the reservoir are presented in Figure 5-37. From April 19th to May 24th, orthophosphate concentrations in the distribution system increased from 1.3 mg P/L to 2.2 mg P/L, corresponding to an increase in reservoir orthophosphate concentrations from 1.3 mg P/L to 1.6 mg P/L. From June 2nd to August 23rd, average orthophosphate concentrations decreased to 1.5 mg P/L, corresponding to a reservoir concentration of 1.0 mg P/L. By October 10th, concentrations in the distribution system reached a maximum of 2.2 mg P/L while the reservoir concentration reached a maximum of 1.9 mg P/L.

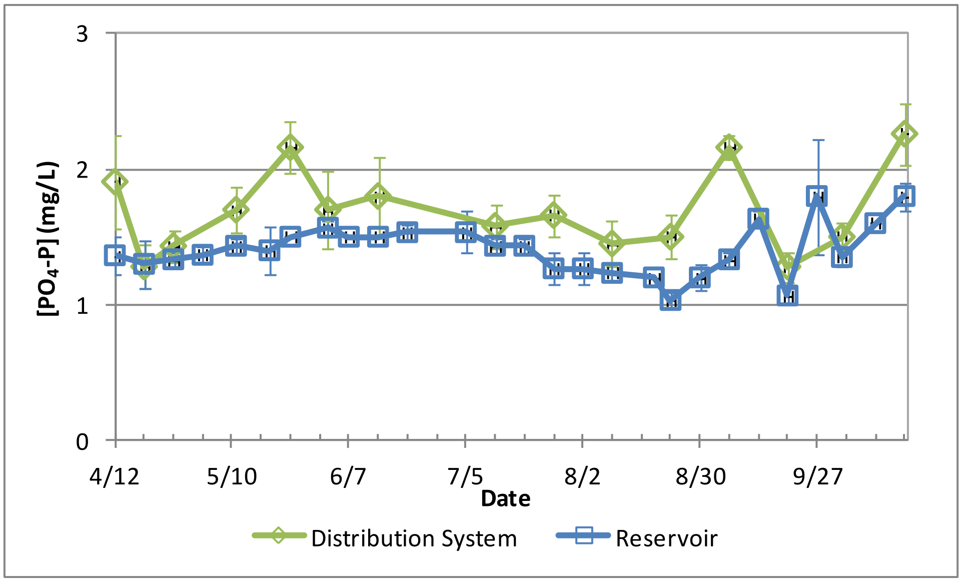

Figure 5-37: Orthophosphate Concentrations in the Distribution System and the Reservoir Surface at Location B

For both ammonia and orthophosphate, concentrations in the distribution system are often greater than concentrations in the reservoir. This may be due to a combination of the following reasons. The distribution system receives reservoir water throughout the night during which algae undergo dark respiration and enter a chemotrophic state for cellular growth. Cellular phosphorus is returned to various organic and inorganic (orthophosphate) forms during respiration. Cellular nitrogen is released as various organic and inorganic (ammonia) forms during respiration, and organic nitrogen undergoes bacterial decomposition and is released as ammonia (Levinton and Waldman, 2006). It is possible that nighttime orthophosphate and ammonia concentrations would be greater than daytime concentrations due to release during respiration and the bacterial decomposition. Also, distribution water is a blend of treated wastewater and reservoir water. As reported in Section 5.1.2, nighttime (12 PM to 7 AM) concentrations of orthophosphate and ammonia from oxidation ditch effluent ranged from 1 mg P/L to 3 mg P/L and 1 mg N/L to 6 mg N/L, respectively. Nighttime oxidation ditch effluents are typically greater than the sampled reservoir concentrations and the addition of plant effluent to reservoir effluent may increase export water concentrations above reservoir concentrations.

In general, dark respiration and the mixing of reservoir water with treated wastewater during export pumping may cause distribution system levels to exceed sampled reservoir levels.

5.4.2 Turbidity

Turbidity was sampled in the distribution system in order to determine the overall water clarity. Turbidity accounts for a wide range of suspended material such as soil particles, algae, and microorganisms, and was a good indicator of potential filter clogging particles. The average turbidity throughout the distribution system is presented in Figure 5-38 with error bars representing the standard deviation of the data. Turbidity increased from 1.2 to 5.5 NTU from April 19th to May 3rd and remained between 5 and 6 NTU until June 21st. From July 5th to August 23rd, turbidity decreased to approximately 3 NTU then increased to greater than 5 NTU from September 6th to September 20th. At the end of the study, the average turbidity decreased to approximately 3.5 NTU. These numbers are consistent with reservoir turbidity. Figure 5-39 presents reservoir turbidity profiles at the beginning of each month throughout the duration of the study. Reservoir turbidity increased from May to June by approximately 3 NTU, then decreased from June to August by 2 NTU.

Distribution water had the lowest turbidity from April to June and the beginning of September, and the highest turbidity from June to the end of August. As discussed in Section 5.2.3, June to August was the time of highest photosynthetic activity.

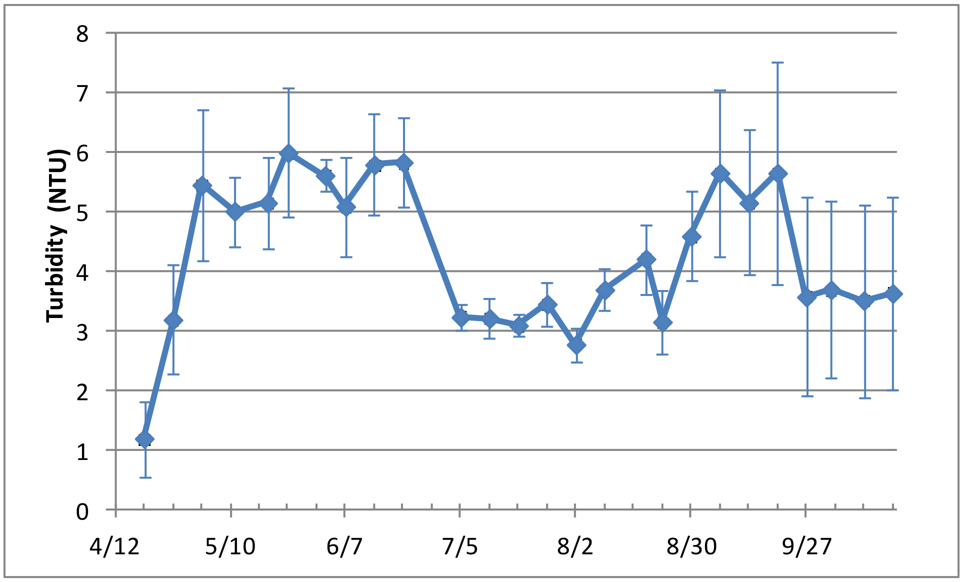

Figure 5-38: Average Distribution System Turbidity throughout Water Quality Study

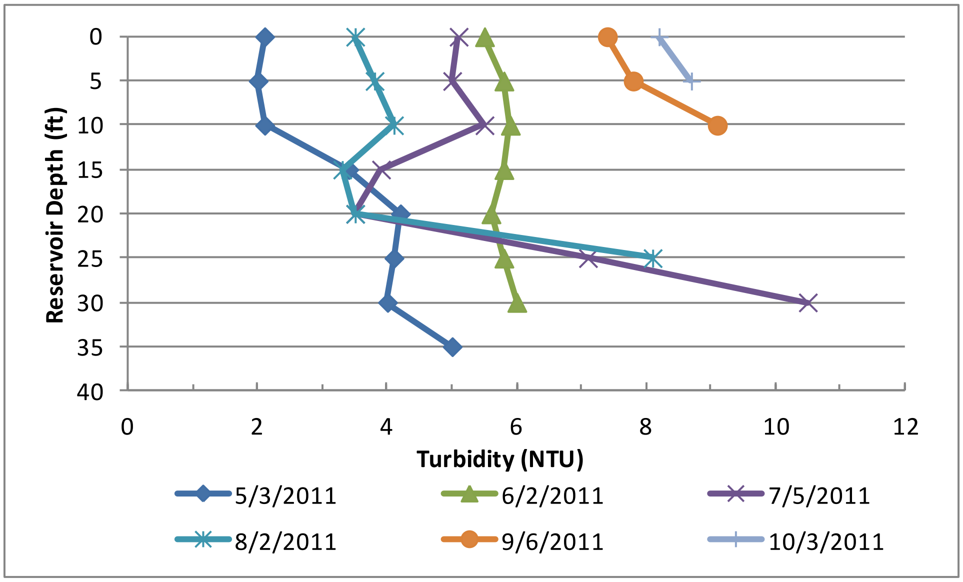

Figure 5-39: Reservoir Turbidity Profile at Various Days throughout Water Quality Study at Location B

5.4.3 Dissolved Oxygen

Due to the high levels of DO in the reservoir, DO was expected to be present in sufficient concentrations in the distribution system. Due to nighttime distribution and dark respiration, DO concentrations in the distribution system were expected to be lower than reservoir concentrations. Average DO concentrations in the distribution system and at the reservoir surface at Location B are presented in Figure 5-40. Concentrations were typically greater than 5 mg O_2/L . DO concentrations in the distribution system decreased from 10.5 to 5.1 mg O_2/L from April 26th to June 7th while reservoir concentrations decreased from 6.2 to 5.0 mg O_2/L. By August 9th, DO in the distribution system increased to 12 mg O_2/L while the reservoir concentration had decreased to 8.1 mg O_2/L. DO in the distribution system reached a minimum average concentration of 4.1 mg O_2/L by September 13th while the reservoir concentration increased to 11.2 mg O_2/L.

From April 26th to June 7th, DO concentrations in the distribution system were greater than reservoir concentrations, despite the increased oxygen demand at night. Due to colder nighttime temperatures, DO saturation concentrations would increase compared to warmer daytime temperatures. Temperature data were not collected at night so it is difficult to determine DO saturation concentration in the reservoir. Table 5-18 shows the difference in daytime high and nighttime low temperatures from April 26th to June 7th. The difference in temperature (10-15 ^{o}C) between day and night suggests it is possible that the upper layers of the reservoir cooled off enough to allow an increase in DO at night. Also, near freezing temperatures at night during April may have inhibited microbial respiration and the consumption of DO.

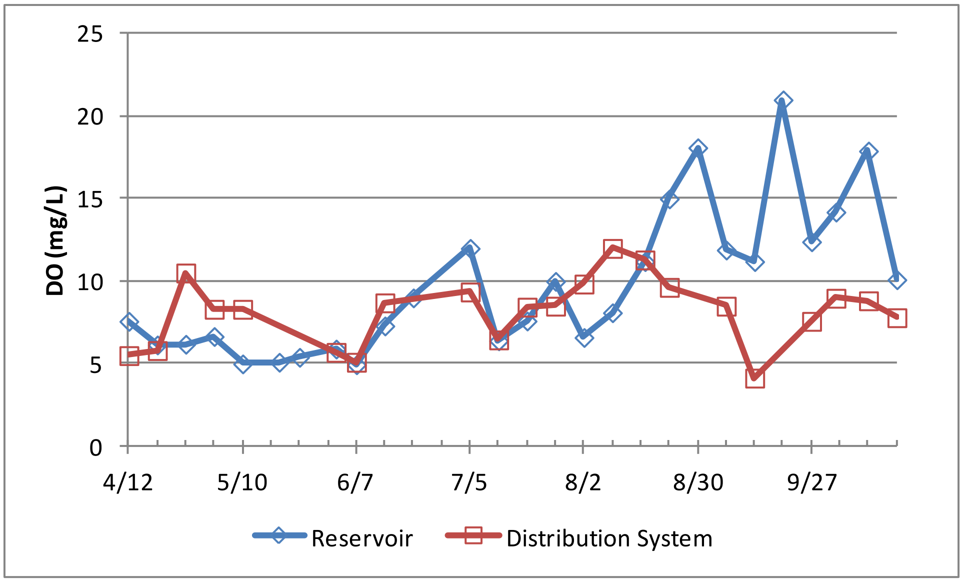

Figure 5-40: Dissolved Oxygen Concentrations in Distribution System and Reservoir

Table 5-18: Maximum and Minimum Air Temperatures

Date	Max Daytime T (^{o}C)	Min Nighttime T (^{o}C)
4/12/2011	17.2	0.6
4/19/2011	20.0	5.6
4/26/2011	15.6	1.7
5/3/2011	22.2	5.6
5/10/2011	20.0	5.0
6/2/2011	15.6	3.9
6/7/2011	22.2	4.4

Chapter 6 Conclusions and Further Research

The utilization of reclaimed wastewater for landscape irrigation has the potential to reduce potable water demands across the United States, especially in arid regions. Currently, the quality of reclaimed water from STMWRF does not meet the quality criteria desired by customers, requiring increased treatment to satisfy end user needs. A variety of water quality assessments, nutrient removal efficiencies, as well as new treatment options were examined in order to determine how current and future operations affect end user water quality.

The first study examined the hourly nutrient treatment efficiency in STMWRF's oxidation ditch. It was found that intermittent aeration resulted in high ammonia and orthophosphate loadings into Huffaker Hills Reservoir. It is thought that continuous operation of the aerators could reduce ammonia and orthophosphate loading by 78% and 40%, respectively. Phosphorus concentrations during off-aeration cycles exceeded maximum influent concentrations due to biological release in the anaerobic environment. In the near future, STMWRF will be implementing a controlled system where aeration is dependent on oxidation ditch ammonia concentrations.

During the distribution season, a reservoir water quality study was conducted in order to assess algae growth and fluctuations in water quality as a result of nutrient-rich wastewater loading. It was found that algae growth was most active from June through August. During this time, pH and DO increased from 7 to 10.5 and 5 to 18 mg O_2/L, respectively. Throughout the distribution season, algae in the reservoir were nitrogen-limited as evidenced by N:P ratios that were typically less than 2. When algae were most active (June through August), ammonia and orthophosphate concentrations decreased from 1.9 to 0 mg N/L and 1.5 to 1.0 mg P/L, respectively. Future research should focus on monitoring algae growth and surface nutrient concentrations in the reservoir to assess the effects of the new controls on the aeration system.

During the reservoir water quality study, a chemical coagulation experiment was constructed to determine the capabilities of alum and $FeCl_3$ for the removal of turbidity from a mixture of plant and reservoir water. The pilot-scale experiment consisted of two gravity driven sand columns which were run in parallel to compare the effects of chemical coagulation and filtration to filtration alone. It was found that as the dose of coagulant increased, the variability in the amount of turbidity removal decreased. $FeCl_3$ performed better than alum, with an average turbidity reduction of approximately 70% at a dose of 28 mg/L. The filtration system utilized at STMWRF consists of continuously backwashed upflow filters which may not directly compare to the downflow filters used in the pilot-scale experiments. In order to determine the removal capabilities of the existing filtration system, a full-scale coagulation experiment should be conducted on the upflow filters throughout the distribution season.

The final study examined the water quality in the Washoe County reclaimed water distribution system. NH_3 and PO_4^{3-} concentrations in the distribution system often exceeded concentrations measured in the reservoir. It is thought that this was due to a combination of algae dark respiration of algae, which releases NH_3 and PO_4^{3-}, and the mixture of oxidation ditch effluent with reservoir water.

This study sought to highlight the problems and potential solutions to the water quality of Washoe County’s reclaimed water distribution system. It is hypothesized that the most efficient and economical method for increasing end-user water quality is through complete aeration of the oxidation ditch at STMWRF. Complete aeration could reduce ammonia loading into the reservoir by approximately 78%. Algal growth in the reservoir is nitrogen limited due to the low N:P ratio, and further reductions in the amount of available nitrogen in the reservoir would further limit algae growth. However, in order to determine the most economical method for improving end-user water quality, a cost-benefit analysis should be performed comparing increased oxidation ditch aeration, reservoir aeration, and the addition of coagulants to the filtration process.

References

Abeliovich, A. & Azov, Y., 1976. Toxicity of ammonia to algae in sewage oxidation ponds. *Applied and Environmental Microbiologyy*, 31(6), pp.801-06.

Asano, T., 1987. Irrigation with Reclaimed Municipal Wastewater. *GeoJournal*, 15(3), pp.273-82.

Bouwer, H., 2002. Integrated Water Management for the 21st Century: Problems and Solutions. *Journal of Irrigation and Drainage Engineering*, 128(4), pp.193-202.

Bruvold, W.H., Olson, B.H. & Rigby, M., 1981. Public Policy for the Use of Reclaimed Water. *Environmental Management*, 5(2), pp.95-107.

Cayana, D.R. et al., 2010. Future dryness in the southwest US and the hydrology of the early 21st century drought. *Proceedings of the National Academy of Sciences*, 107(50), pp.21271-76.

Chen, C.Y. & Durbin, E.G., 1994. Effects of pH on the growth and carbon uptake of marine phytoplankton. *MARINE ECOLOGY PROGRESS SERIES*, 109, pp.83-94.

Cole, J.J., 1982. Interactions Between Bacteria and Algae in Aquatic Ecosystems. *Annual Review of Ecology and Systematics*, 13, pp.291-314.

Devitt, D.A. et al., 2005. Water Quality Changes in Golf Course Irrigation Ponds Transitioning to Reuse Water. *Hort Science*, 40(7), pp.2151-56.

DNR, W., 2006. *Wastewater Fractionation*. [Online] Available at: http://dnr.wi.gov/org/water/wm/ww/biophos/3fract.htm [Accessed 23 February 2012].

Friedman, A.A., Peaks, D.A. & Nichols, R.L., 1977. Algae Separation from Oxidation Pond Effluents. *Water Pollution Control Federation*, 49(1), pp.111-19.

Gleick, P.H., 2000. A Look at Twenty-first Century Water Resources Development. *Water International*, 25(1), pp.127-38.

Golueke, C.G. & Oswald, W.J., 1965. Harvesting and Processing Sewage-Grown Planktonic Algae. *Water Pollution Control Federation*, 37(4), pp.471-98.

Google, M., 2012. *Google Maps*. [Online] Available at: http://www.maps.google.com [Accessed March 2012].

Goronszy, M.C., 1979. Intermittent Operation of the Extended Aeration Process for Small Systems. *Water Pollution Control Federation*, 51(2), pp.274-87.

Harrington, G.W., Noguera, D.R., Bone, C.C. & Kandou, A.I., 2003. *Ammonia from chloramine decay*. American Water Works Association.

Hipkin, C.R. & Syrett, P.J., 1977. Some Effects of Nitrogen-Starvation on Nitrogen and Carbohydrate Metabolism in Ankistrodesmus braunii. *Planta*, 133, pp.209-14.

Hulett, J., 2012. *Engineer*. Reno: Washoe County.

Insel, G., Artan, N. & Orhon, D., 2005. Effect of Aeration on Nutrient Removal Performance of Oxidation Ditch Systems. *ENVIRONMENTAL ENGINEERING SCIENCE*, 22(6), pp.802-15.

Jansson, M., 1988. Phosphate uptake and utilization by bacteria and algae. *Hydrobiologia*, (170), pp.177-89.

Jjemba, P.K. et al., 2010. Regrowth of Potential Opportunistic Pathogens and Algae in Reclaimed Water Distribution Systems. *Applied and Environmental Microbiology*, 76(13), pp.4169-78.

Kessler, E., Arthur, W. & Brugger, J.E., 1957. The Influence of Manganese and Phosphate on Delayed Light Emission, Fluorescence, Photoreduction and Photosynthesis in Algae. *Archives of Biochemistry and Biophysics*, 71, pp.326-35.

Levinton, J.S. & Waldman, J.R., 2006. *The Hudson River Estuary*. New York, New York: Cambridge University Press.

Maurer, M., Gujer, W., Hany, R. & Bachmann, S., 1997. Intracellular carbon flow in phosphorus accumulating organisms from activated sludge systems. *Water Research*, 31(4), pp.907-17.

Moss, B., 1973. The Influence of Environmental Factors on the Distribution of Freshwater Algae: An Experimental Study: II. The Role of pH and the Carbon Dioxide-Bicarbonate System. *Journal of Ecology*, 61(1), pp.157-77.

Naghavi, B. & Malone, R.F., 1986. Algae Removal by Fine Sand/Silt Filtration. *Water Resources*, 20(3), pp.377-83.

Oswald, W.J. et al., 1957. Algae in Wastewater Treatment. *Water Environment Federation*, 29(4), pp.437-57.

Paasche, E., 1971. Effect of Ammonia and Nitrate on Growth, Photosynthesis, and Ribulosediphosphate Carboxylase Content on Dunaleilla tertiolecta. *Physiology of Plants*, 25, pp.294-99.

Raschke, R.L., 1970. Algal Periodicity and Waste Reclamation in a Stabilization Pond Ecosystem. *Water Pollution Control Federation*, 42(4), pp.518-30.

Rhee, G.-Y. & Gotha, I.J., 1980. OPTIMUM N: P RATIOS AND COEXISTENCE OF PLANKTONIC ALGAE. *ournal Of Phycology*, 16(4), pp.486-89.

Rittmann, B.E. & McCarty, P.L., 2001. *Environmental Biotechnology: Principals and Applications*. New York, NY: McGraw-Hill.

Romanski, J., Heider, M. & Wiesmann, U., 1997. Kinetics of Anaerobic Phosphate Release and Substrate Uptake in Enhanced Biological Phosphorus Removal in Synthetic Wastewater. *Water Resources*, 31(12), pp.3137-45.

Ryther, J.H., 1956. Photosynthesis in the Ocean as a Function of Light Intensity. *Limnology and Oceanography*, 1(1), pp.61-70.

Sorokin, C. & Krauss, R.W., 1956. THE EFFECTS OF LIGHT INTENSITY ON THE GROWTH RATES OF GREEN ALGAE. *Plant Physiology*, 32(2), pp.109-13.

Tchobanoglous, G., Burton, F.L. & Stensel, H.D., 2003. *Wastewater Engineering Treatment and Reuse*. 4th ed. New York, New York: McGraw-Hill.

Toze, S., 2005. Reuse of effluent water—benefits and risks. *Agricultural Water Management*, 80, pp.147-59.

Van Vuuren, L.R.J. & Van Vuuren, F.A., 1965. Removal of Algae from Wastewater Maturation Pond Effluent. *Water Pollution Control Federation*, 37(9), pp.1256-62.

Wyatt, N.B. et al., 2011. Critical Conditions for Ferric Chloride-Induced Flocculation of Freshwater Algae. *Biotechnology and Bioengineering*, 109, pp.493-501.